processes

MDPI

Article

Research on the Prediction Method of the Areas of Fluorine Chemical Pipeline Susceptible to Erosion

Zhou Fang [1,*], Puan Shi [1], Junjie Fu [1], Ce Song [2], Jun Yuan [2] and Jin Deng [2]

[1] College of Mechanical and Electrical Engineering, Beijing University of Chemical Technology, Beijing 100029, China; 2020200637@buct.edu.cn (P.S.); jjfu@buct.edu.cn (J.F.)
[2] China Special Equipment Inspection and Research Institute (CSEI), Beijing 100029, China; songce2022@126.com (C.S.); 18910756539@163.com (J.Y.); 18600298584@163.com (J.D.)
* Correspondence: zhoufang@buct.edu.cn

Abstract: A prediction method applicable to erosion-prone areas of fluorine chemical pipelines is herein proposed. By summarizing the common working conditions in the fluorine chemical industry, a computational fluid dynamics (CFD) model for industrial pipelines is established, and three-dimensional numerical calculations of the flow field in the pipelines are carried out to analyze the characteristics of the hydrodynamic parameters and phase distribution in the flow field, as well as the erosion rate distribution in different areas of the pipelines. The areas in the pipeline that are susceptible to erosion are predicted based on the results. The method has universal applicability and has been applied in many large petrochemical companies. It achieves the function of predicting the areas of severe pipeline erosion in a scientifically sound manner. This paper also details the application of the method in a distillation oil and gas pipeline of a large oil and gas company in western China.

Keywords: fluorine chemical industry; dangerous point; computational fluid dynamics; erosion

Citation: Fang, Z.; Shi, P.; Fu, J.; Song, C.; Yuan, J.; Deng, J. Research on the Prediction Method of the Areas of Fluorine Chemical Pipeline Susceptible to Erosion. *Processes* **2022**, *10*, 657. https://doi.org/10.3390/pr10040657

Academic Editor: Chi-Min Shu

Received: 15 February 2022
Accepted: 25 March 2022
Published: 28 March 2022

1. Introduction

The fluorine chemical industry has a unique position in the chemical production industry due to its wide range of categories and industrial relevance [1–5]. The materials between different processes in the fluorine chemical industry are generally transported through pipelines, and the pipelines of fluorine chemical enterprises are shown in Figure 1. Due to most of the production materials and products being transported in fluorine chemical pipelines being toxic and highly corrosive dangerous chemicals, once the pipelines are perforated and leaked, significant losses to the production enterprises will result. Therefore, the safety performance of pipelines plays an important role in fluorine chemical production.

Erosion is one of the important causes of wall thinning and perforation, due to erosion resulting in perforated pipe fittings, as shown in Figure 2. In recent years, the trend of deterioration of pipelines carrying dangerous media is very obvious, and the wall erosion thinning situation is very serious, increasing safety risks.

In order to prevent pipe wall thinning and perforation, it is necessary to stop the whole pipeline for safety monitoring or maintenance during the production process. This increases production costs and makes it difficult to ensure that accidents do not occur. By predicting and studying the risk points in the erosion-prone areas of the pipelines, we can get the distribution of areas of the pipelines with higher risk of erosion.

At present, scholars mainly focus on pipeline risk assessment and life prediction technology research for pipeline failure prediction and establish the failure risk calculation formula. Before the pipeline risk assessment life prediction, the limiting hazard factors of the evaluated pipeline should be identified, and the relevant data should be comprehensively analyzed.

Figure 1. Fluorochemical pipeline.

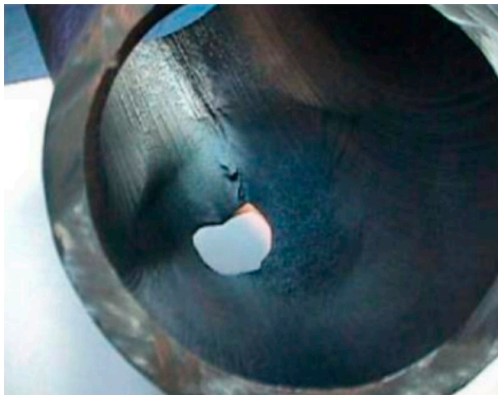

Figure 2. Elbow perforated by erosion.

In terms of the degree of risk assessment, it can be divided into qualitative risk analysis methods represented by expert scoring method, risk evidence method and fault tree method. This type of method is simple to operate but the results obtained are relatively crude. The quantitative analysis method is represented by the probabilistic risk assessment (PRA) method. This type of method is complex and requires a large database to support the analysis process. There are also semi-quantitative risk evaluation methods such as risk index-based risk evaluation methods [6–14].

Specifically, pipeline failure prediction methods include the following:

(1) Electrochemical analysis method [6,7]: This method is an important way to analyze kinetic information of the electrochemical corrosion process. This method is an important way to analyze the kinetic information of electrochemical corrosion processes. This method predicts the corrosion of materials by analyzing the corrosion pattern of CO_2 on steel in the environment of oil and gas aggregation, the corrosion rate of metallic steel, and the electrochemical characteristics of corrosion of steel materials under the influence of temperature CO_2. However, this method only considers the corrosion effect of CO_2 and material, ignoring the influence of other corrosive media on pipelines, which is not applicable to the fluorine chemical process.

(2) Reliability function analysis method [8,9]: The statistical distribution law of the probability of erosion failure is given by the statistics of the erosion defect size and erosion development law. The risk of the pipeline is evaluated, and the maintenance cycle of the pipeline is determined.

(3) Probability statistics method [10,11]: This method is based on the assumption of linear development of long-term erosion rates and introduces normal and non-normal distributions among the variables associated with erosion defects. The pipeline erosion data were analyzed by probability statistics, and a reasonable mathematical model of random variables was established to obtain the probability distribution. Statistics, analysis and calculation of erosion-related parameters are performed.

The above two methods need to be based on a large amount of historical data. Although the application of the corrosion situation and the historical database matching the pipeline is better, the actual working conditions of the pipeline, structure and environmental changes make the actual results differ too much from the theoretical results.

(4) Artificial neural network method [12]: The BP network is used to judge and predict the hazardous media pipelines. The known sample set of this method consists of various corrosion factors and corrosion test results of pipelines in long-term operation. Through the self-learning habit of neural networks, knowledge is acquired and then predicted for the unknown system, which eventually leads to the number of years that the new system can be used. However, the use of artificial neural network technology is difficult, the judgment process is complex and the operability is poor.

(5) Gray system theory method [13,14]: By fitting the actual statistics of erosion rate and erosion depth of hazardous media pipelines dynamically, the corresponding gray differential method and gray time correspondence function are established to discover the law of pipeline erosion rate and erosion depth change with time. However, due to the small sampling volume and simple calculation, the analytical parameters can only yield the relationship between erosion rate and erosion depth.

In this study, a computational fluid dynamics (CFD) model of an industrial pipeline was developed. Three-dimensional numerical calculations of the flow field in the pipeline were carried out. The hydrodynamic parameters and phase distribution characteristics in the flow field were analyzed. The erosion rate distributions in different regions of the pipeline were provided. Weak and vulnerable areas of industrial pipelines were predicted. Thus, a method for predicting the erosion areas of pipelines was established.

The following influencing factors must be considered in the process of calculating the results from the flow field to the predicted erosion section to ensure that the results are analyzed and processed in a reasonable manner to produce an accurate erosion area.

(1) The initial wall thickness of the pipe: In the actual industrial pipelines, elbow, tee and other pipe fittings due to the impact of processing links, the initial wall thickness distribution is not uniform. For example, the initial wall thickness of the outside of the elbow processed using the hot-drawing process is the smallest, while the initial wall thickness of the elbow is measured inside the largest; the initial wall thickness of the straight pipe of the tee is smaller on both sides of the connection with the branch pipe. The above-mentioned areas are often mistaken for the smaller initial wall thickness of the erosion thinning serious areas. In addition, the same number of different areas of the industrial pipelines often have a different wall thickness, in the judgment of the wall thinning at the need and erosion rate comprehensive consideration. Therefore, if the initial wall thickness of the pipe is not consistent, it is necessary to make a comprehensive judgment. In the prediction of industrial pipeline vulnerable parts, the same specification of the pipe (such as comparison of the pipe to ensure that the pipe is the same specification, comparison of the elbow at the same time than the same part of the elbow, etc.), the reference significance of the erosion calculation results more significant.

(2) The effect of an erosion etching mechanism: The erosion distribution maps provided in the following sections are mainly based on impact velocity calculations. Impact angle on the impact rate of erosion the impact angle is to cause the thinning position of small-scale offset. In the case of elbows, for example, the high impact rate and near-optimal impact angle at the exit of the elbow make it a hazardous point. Although the

impact angle has an effect on the erosion distribution based on the impact velocity, this effect only leads to a small-scale shift in the thinning location, which is limited to the vicinity of the tube being analyzed. Therefore, the trade-off between inspection and calculation costs is that the erosion calculation identifies as few limited areas on critical fittings as possible, and that these areas are inspected in detail by the inspector to compensate for the calculation bias caused by the high calculation costs.

(3) The influence of the calculation method: pipelines flow field calculation can be used for transient multiphase flow, steady-state two-phase flow coupling, steady-state two-phase flow discrete, steady-state single-phase flow and other calculation methods; the calculation accuracy and calculation of the consumption time in order to reduce.

2. Numerical Calculation Method

2.1. Theories of Erosion

Until now, there has been no mature theory to scientifically explain the erosion process, and the working conditions of fluorine chemical industry are more complex, with temperatures as low as −196 °C and as high as over 500 °C, involving many corrosive media (Table 1). In the numerical calculation of classical fittings, scholars studying fluorine chemical industry media mostly use the K-ε model as the turbulence model, mainly using the Standard K-ε model proposed by Launder [15] or the RNG K-ε [16] model proposed by Orzag for numerical simulation studies.

Table 1. Working conditions of fluorinated chemical industry.

No.	Specific Content	Temperature (°C)	Pressure (MPa)	Material	Flow Rate	References
1	Acetylene pipeline (96% acetylene) of a fluorine chemical plant in Changshu, China	Room temperature	0.3	304 stainless steel	/	[15]
2	Reflux tower condenser of a fluorochemical plant in Changshu, China	Shell range 35/tube range 15	Shell range 0.7/tube range 2.11	Shell course 16 MnDR/tube course 304L	/	[15]
3	AHF production process	Phase I: 100~120 Phase II: 160~200	/	/	/	[16]
4	HF acid regeneration tower (alkylation)	150	0.45	Monel400	/	[17]
5	Alkyl benzene HF acid regeneration tower heater (shell process for hot oil, tube process for HF plus hydrocarbon)	215~265	/	Monel400	Operation flow rate: 16.520 m^3/h	[18]
6	Alkyl benzene HF regeneration tower	200	/	Monel400	3.173 kg/cm^2	[19]
7	Sodium fluorosilicate to sodium fluoride method	8495	≤0.148	/	Agitator stirring rate: 4 m/s	[16]
8	Hydrogen fluoride cooling crystallization kettle	In-vessel: <90/ In-jacket: 32	Inside the container: 0/Inside the jacket: 0.02~0.03	/	/	[20]

Table 1. *Cont.*

No.	Specific Content	Temperature (°C)	Pressure (MPa)	Material	Flow Rate	References
9	Soda ash production method of sodium fluoride	Temperature of reactor: 84~95	≤0.148	/	/	[16]
10	Melt production of iodine pentafluoride	Fine iodine melting temperature: 113~150	Temperature of fine iodine melting. 300 kpa	/	/	[16]
11	Steel can packaging for fluorine gas	21	≤2.86 (in China: ≤0.5)	/	/	[16]
12	Packaging of sulfur hexafluoride	21.1	4	30 CrMo or aluminum alloy	/	[16]
13	Electrolytic production process of nitrogen trifluoride	126~160	Atmospheric pressure ~0.3445 (gauge pressure)	/	/	[16]
14	Electrochemical production process of ammonia fluoride	95~150	0.1	/	/	[16]
15	Showa Denko Co. CF_4 preparation process by two-stage cyclic reaction method	First, second reactor: 370	First, second reactor: 1.5	/	/	[16]
16	Membrane Separation Method for Perfluorocarbon Production at Air Liquide USA	Adsorption temperature 30~100	Adsorption pressure: 0.3~2.0	/	/	[16]
17	Production of vinylidene fluoride by deHCL of HCFC-142b	VDF distillation column condensing temperature −15	/	/	/	[21]
18	Production of HCFC-22	Temperature of the reactor 30	Operating pressure: 0.8	/	Water flow velocity 1.5 m/s; F152a flow rate 15 m/s	[18]
19	Hexafluoropropylene distillation column	T-1: −16 T-2: 5 T-3: 27 T-4: 20 T-5: 17	T-1: 1.3 T-2: 1 T-3: 0.75 T-4: 0.55 T-5: 0.35	/	Feed volume 516.4 kg/h	[19]
20	Production process of PTFE	HCFC-22: Predicted temperature	/	Iconel	/	[20]
21	R142b non-diluted thermal cracking	700~900	1	Stainless Steel	Feed volume: 650~800 mL/min	[21]

Table 1. *Cont.*

No.	Specific Content	Temperature (°C)	Pressure (MPa)	Material	Flow Rate	References
22	1-Chloro-1,1-dichloroethane reaction distillation process	Temperature of the tower kettle: 130	Pressure at the top of the tower: 1.6	/	VDC: 0.22 HCFC-141b: 159.9 kg/h HCFC-142b: 502.0 kg/h HFC-143a: 37.69 kg/h HCL: 205.3 kg/h HF: 104.3 kg/h	[22]
23	Production process of hexafluoropropylene	Sensitive version shows temperature: 313~320	/	/	Feed volume: 174 kmol/h	[23]

Most of the research is only based on a specific working condition to study the effect of different factors on the erosion results. According to literature research, the erosion behavior of the pipe is mainly influenced by the medium flow rate in the pipe and the geometry of the pipe fittings by a few inches.

In this study, elbows, reducers, valves and tees will be investigated, and the study of elbows has been mentioned in other studies in this laboratory [24]. In this paper, we will conduct a specific study on the erosion in a typical fluorine chemical process. According to the research, the medium flow rate in the tube and the geometry of the pipe fittings (such as the pipe diameter, elbow ratio and valve opening) have a more obvious effect on the erosion of the pipe fittings. Therefore, low flow rate (0.1 m/s–1 m/s), pipe diameter ratio on the tee tube, reducer model, low flow rate, pipe diameter, opening and taper on the valve model of the impact caused by erosion is studied.

The field research was carried out through the Quzhou Juhua plant in Zhejiang Province, and the specific situation of the key device F22 was selected. Among them, the reaction temperature range of R22 reactor is 70~100 °C, the pressure range is 1–2 MPa and the main medium is chloroform. Therefore, chloroform was used as the in-pipe medium to study the effect of different piping characteristics and changes in various parameters at different medium flow rates on erosion.

2.2. Modeling Method

2.2.1. Basic Control Equations

Fluid dynamics follows the basic laws of physics: conservation of mass, conservation of momentum and conservation of energy. The expressions of the three equations are shown in Formula (1)–(6).

(1) The mass conservation equation.

$$\frac{\partial \rho}{\partial t} + \frac{\partial(\rho u_x)}{\partial_x} + \frac{\partial(\rho u_y)}{\partial_y} + \frac{\partial(\rho u_z)}{\partial_z} = 0 \quad (1)$$

In the formula:

ρ—The fluid density in kg/m^3;

u_x—The velocity vectors of fluid velocity along the x directions in m/s;

u_y—The velocity vectors of fluid velocity along the y directions in m/s;

u_z—The velocity vectors of fluid velocity along the z directions in m/s;

For incompressible fluids, where ρ is a constant, Formula (1) can be rewritten as Formula (2).

$$\frac{\partial u_x}{\partial_x} + \frac{\partial u_y}{\partial_y} + \frac{\partial u_z}{\partial_z} = 0 \tag{2}$$

(2) Conservation of momentum equation:

x-direction:

$$\frac{\partial(\rho u_x)}{\partial t} + \nabla(\rho u_x \cdot \overline{u}) = -\frac{\partial p}{\partial_x} + \frac{\partial \tau_{xx}}{\partial x_x} + \frac{\partial \tau_{yz}}{\partial x_y} + \frac{\partial \tau_{zx}}{\partial x_z} + \rho f_x \tag{3}$$

y-direction:

$$\frac{\partial(\rho u_y)}{\partial t} + \nabla(\rho u_y \cdot \overline{u}) = -\frac{\partial p}{\partial_y} + \frac{\partial \tau_{xy}}{\partial x_x} + \frac{\partial \tau_{yy}}{\partial x_y} + \frac{\partial \tau_{zy}}{\partial x_z} + \rho f_y \tag{4}$$

z-direction:

$$\frac{\partial(\rho u_z)}{\partial t} + \nabla(\rho u_z \cdot \overline{u}) = -\frac{\partial p}{\partial_z} + \frac{\partial \tau_{xz}}{\partial x_x} + \frac{\partial \tau_{yz}}{\partial x_y} + \frac{\partial \tau_{zz}}{\partial x_z} + \rho f_z \tag{5}$$

In the formula:

P—The static pressure, in N;

τ_{xx} τ_{xy} τ_{xz}—The stress components acting in the x, directions, in Pa;

τ_{yx} τ_{yy} τ_{yz}—The stress components acting in the y, directions, in Pa;

τ_{zx} τ_{zy} τ_{zz}—The stress components acting in the z, directions, in Pa;

f_x—The unit mass forces in the x directions, in N;

f_y—The unit mass forces in the y directions, in N;

f_z—The unit mass forces in the z directions, in N;

(3) Energy conservation equation:

$$\frac{\partial(\rho T)}{\partial t} = div(\rho u T) = div\left(\frac{k}{C_\rho} grad T\right) + S_T \tag{6}$$

Expanded as Formula (7).

$$\begin{gathered}\frac{\partial(\rho T)}{\partial t} + \frac{\partial(\rho u_x T)}{\partial x} + \frac{\partial\left(\rho u_y T\right)}{\partial y} + \frac{\partial(\rho u_z T)}{\partial z} = \\ \frac{\partial}{\partial x}\left(\frac{k}{C_\rho}\frac{\partial T}{\partial_x}\right) + \frac{\partial}{\partial y}\left(\frac{k}{C_\rho}\frac{\partial T}{\partial_y}\right) + \frac{\partial}{\partial z}\left(\frac{k}{C_\rho}\frac{\partial T}{\partial_z}\right)\end{gathered} \tag{7}$$

In the formula:

C_ρ—The constant pressure specific heat capacity in J/(kg*K);

T—The fluid temperature in K;

k—The fluid heat transfer coefficient;

S_T—The viscous dissipation term.

2.2.2. Turbulence Models

The standard K-ε model was proposed in 1972 and is used in FLUENT calculations for general engineering due to its wide applicability. For flows with small Reynolds numbers, the model is not applicable. Therefore, the model can only be used when the fluid is in a fully turbulent state. In the standard K-ε model, the K equation and the turbulent kinetic energy dissipation ε equation are shown in Formula (8) and Formula (9), respectively.

Turbulent pulsation kinetic energy equation (K equation).

$$\rho\frac{Dk}{Dt} = \frac{\partial}{\partial x_i}\left[\left(\mu_l + \frac{\mu_T}{\sigma_k}\right)\frac{\partial k}{\partial x_i}\right] + G_k + G_b - \rho\varepsilon \tag{8}$$

Turbulent kinetic energy dissipation equation (ε equation).

$$\frac{Dk}{Dt} = \frac{\partial}{\partial x_i}\left[\left(\mu_l + \frac{\mu_T}{\sigma_k}\right)\frac{\partial k}{\partial x_i}\right] + C_{1s}\frac{\varepsilon}{k}(G_k + C_{3\varepsilon}G_b) - C_{2s}\rho\frac{\varepsilon^2}{k} \quad (9)$$

In the formula:
μ_l—The laminar viscosity coefficient;
μ_t—The turbulent viscosity coefficient;
$\mu_t = \rho C_\mu \frac{\varepsilon^2}{k}$;
G_k—The turbulent kinetic energy generated by the laminar velocity gradient, in J;
G_b—The kinetic energy of turbulence generated by buoyancy, in J.
σ_k—The empirical constants, In FLUENT, the empirical constants are usually $\sigma_k = 1.0$;
C_{1s}—The empirical constants, in FLUENT, the empirical constants are usually $C_{1s} = 1.44$;
C_{2s}—The empirical constants, in FLUENT, the empirical constants are usually $C_{2s} = 1.92$;
C_{3s}—The empirical constants, in FLUENT, the empirical constants are usually $C_{3s} = 0.09$;
σ_s—The empirical constants, in FLUENT, the empirical constants are usually $\sigma_s = 1.3$.

2.3. Simulation Calculation Method Verification

In this paper, Standard K-ε model is chosen as the turbulence calculation model and SIMPLE algorithm is chosen as the algorithm [24]. In order to verify whether the selected turbulence model, algorithm and mesh division are reasonable, a comparison with what other scholars have studied is made to ensure the reliability of this study. The study by Du [25] is a multi-phase mixed transmission pipeline 90° bend erosion damage stress analysis, which is similar to the selected working conditions in this paper.

2.3.1. Modeling and Meshing

The elbow in the study of Du [25] was selected as the calculation model for this verification. The model diagram of the study is shown in Figure 3. The 3D model of the elbow is shown in Figure 4. The number of meshing is 1 million. The mesh division is carried out by the block method, and the wall mesh is refined. While ensuring the calculation accuracy of the calculation area, the calculation volume of other non-focused calculation areas is reduced and the calculation cycle is shortened. Figure 5 shows the mesh division of the elbow.

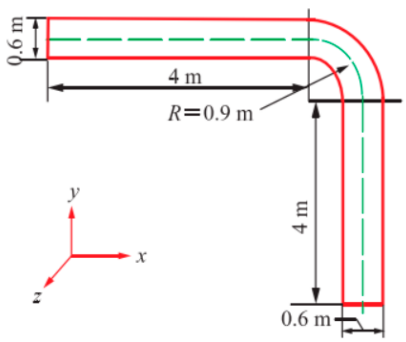

Figure 3. The model diagram of the elbow in references.

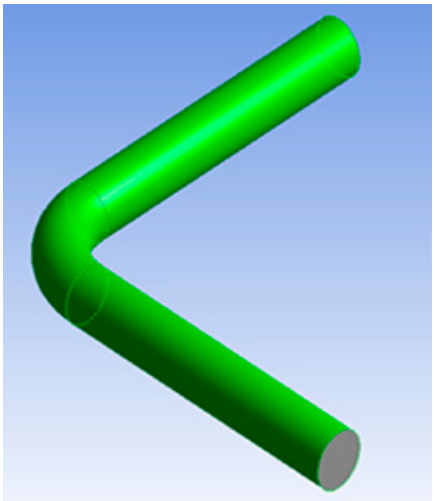

Figure 4. 3D model of the elbow.

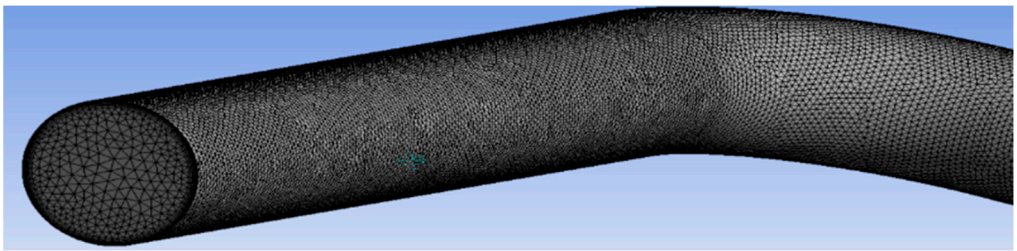

Figure 5. The mashing result.

2.3.2. Boundary Condition Setting

The boundary conditions are shown in Table 2.

Table 2. The boundary conditions of the simulation model.

Inlet flow rate	1.5 m/s	Outlet pressure	0 MPa
Turbulence model	Standard K-ε	Temperature	−1 °C
Liquid density	998 kg/m^3	Liquid viscosity	0.001003 pa*s
Gas density	0.554 kg/m^3	Gas viscosity	0.00025 pa*s
Oil density	875.153 kg/m^3	Oil viscosity	27.87121 pa*s
Oil water content	28%	Oil gas content	2%
Mixed phase density	847.663 kg/m^3	Mixed phase viscosity	0.02 pa*s

2.3.3. Simulation Calculation Method Verification

The above models and parameters were used for numerical simulation calculations. Figure 6 shows the calculation results of the numerical simulation method in this paper. Figure 7 shows the numerical simulation results from the literature.

The velocity clouds and wall shear stress clouds obtained from the calculations are compared with the results in Du [25].

The comparison shows that in the velocity cloud diagram, the medium flow rate near the inner wall surface of the elbow is the largest, and the medium flow rate near the outer wall surface is the smallest. The pressure cloud and the elbow near the inner arch wall pressure is the smallest, and even negative pressure, and near the outer arch wall pressure is the largest. In the wall shear stress cloud, the maximum shear stress is distributed at the two cheeks of the elbow, and the relatively large stress is distributed at the wall of the outer arch downstream of the elbow and the wall of the inner arch upstream of the elbow. It is in full agreement with the research results.

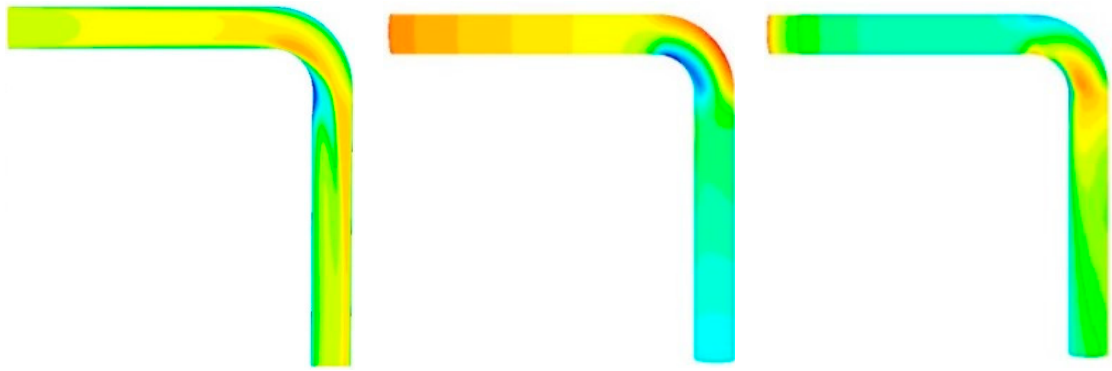

(**a**) (**b**) (**c**)

Figure 6. Calculation results of numerical simulation method; (**a**) Velocity cloud; (**b**) Pressure cloud; (**c**) Wall shear stress cloud.

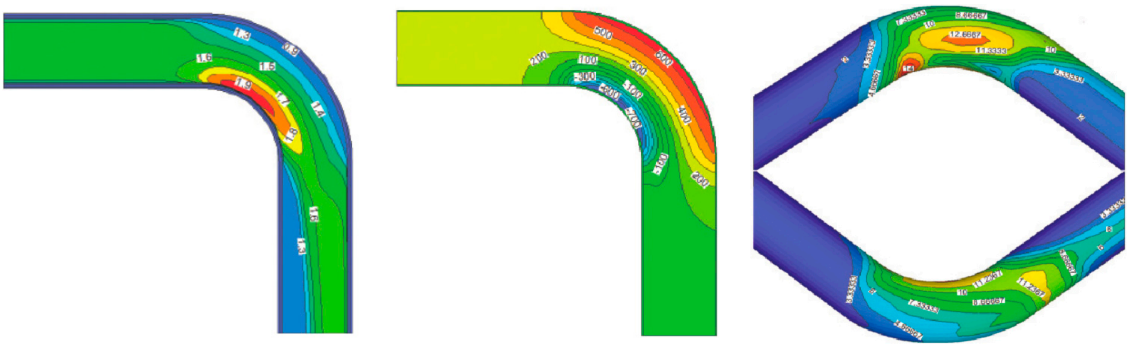

(**a**) (**b**) (**c**)

Figure 7. Calculation results of numerical simulation method in references; (**a**) Velocity cloud; (**b**) Wall shear stress cloud; (**c**) Wall shear stress cloud.

2.4. Prediction Study of Erosion-Prone Areas of the Reducer

2.4.1. Modeling and Meshing

GEOMETRY module is used to model the reducer, and MESH module is used to divide the reducer model mesh. The model diagram of the reducer is shown in Figure 8, and the 3D model diagram of the reducer is shown in Figure 9.

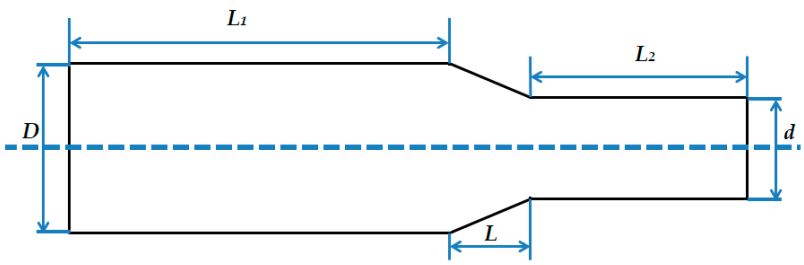

Figure 8. The model diagram of reducer.

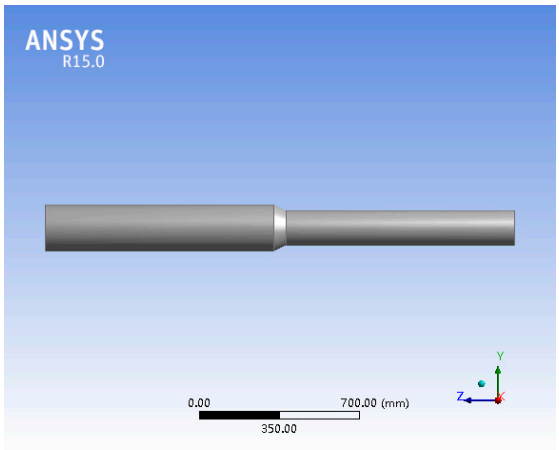

Figure 9. The 3D model diagram of the reducer.

In Figure 8, end D is the fluid inlet end and end d is the fluid outlet end. The direction of fluid flow in the pipe follows the direction of decreasing pipe diameter (from left to right), and L_1 and L_2 are the lengths of the inlet and outlet pipes of the reducer, respectively. To eliminate the influence of the inlet and outlet of the pipe on the results of the erosion study, $L_1 = L_2 = 1000$ mm is taken.

D is the entrance diameter of the reducer, d is the exit diameter of the reducer and L is the length of the tapered pipe. From the length of the tapered pipe and the entrance and exit diameters, the taper k of the tapered pipe can be obtained. The formula for calculating the taper k of the tapered pipe is as in Formula (10).

$$k = (D - d)/L \tag{10}$$

The mesh result is shown in Figure 10. The fine mesh division is performed to ensure that the influence of the mesh on the numerical simulation results is within an acceptable range. The mesh shape is chosen as a triangular mesh with 10 boundary layers, an incremental index of 1.2 and a maximum mesh width of 6 mm.

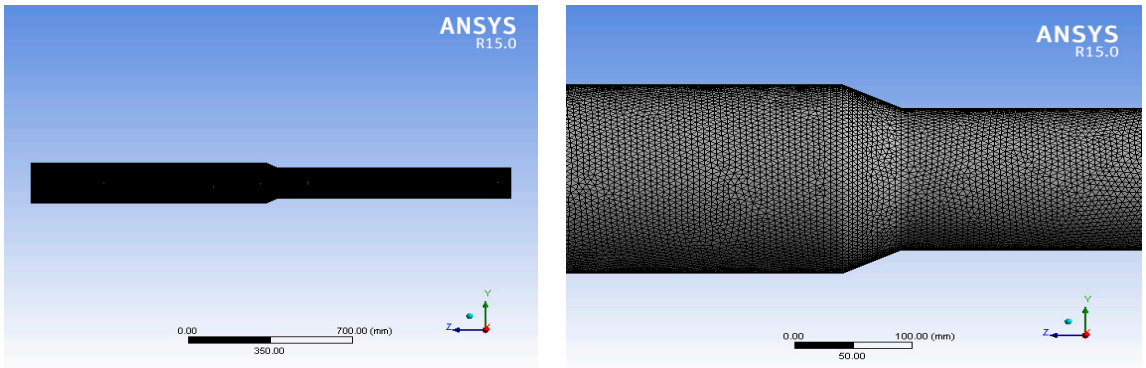

(**a**) (**b**)

Figure 10. The mashing result. (**a**) Overall view; (**b**) Partial view.

2.4.2. Boundary Condition Setting

According to the actual working conditions on site, the reaction temperature range is 70~100 °C, and the main medium in the reactor is chloroform. The pipe diameter size of the two fittings is taken as 50~200 mm according to the common specifications, based on the actual working conditions of Zhejiang Juhua plant and modified according to the fluorine chemical working conditions summarized in Table 1. The pressure difference between the import and export of the fittings is taken as 1 MPa, i.e., the pressure range is 1~2 MPa, and

the mass flow rate in the working conditions is converted into the flow rate according to the pipe diameter. The flow rate range of the numerical simulation working conditions is taken as 0.1~1 m/s.

Chloroform single medium is chosen as the medium in the pipe for calculation. Considering the influence of gravity on pipe erosion, the gravity direction is set along the Y axis, and the gravity value is taken as -9.81 m/s^2. The medium in the pipe is chloroform single flow, the density of chloroform is taken as 1480 kg/m^3, the viscosity is taken as 0.00053 Pa*s; the inlet pressure is taken as 1 × 106 Pa. The medium parameters of the reducer are shown in Table 3.

Table 3. Media parameters of the simulation model.

Density of the Medium in the Pipe kg/m^3	Viscosity of the Medium in the Pipe Pa*s	Pressure of the Medium at the Inlet Pa
1480	0.00053	1,000,000

According to the actual situation, to analyze the effect of low flow rate on erosion, the inlet flow rate is taken as 0.1 m/s, 0.2 m/s, 0.3 m/s, 0.4 m/s, 0.5 m/s, 0.6 m/s, 0.7 m/s, 0.8 m/s, 0.9 m/s and 1 m/s. To study the effect of taper of conical pipe on erosion, the inlet pipe diameter is taken as 200 mm and the outlet pipe diameter is taken as 130 mm, 140 mm, 150 mm, 160 mm, 170 mm. The corresponding taper is 1.4, 1.2, 1.0, 0.8, 0.6. 130 mm, 140 mm, 150 mm, 160 mm and 170 mm, corresponding to the taper of 1.4, 1.2, 1.0, 0.8, 0.6. The pipe fittings calculated in this paper are all round pipes, so the inlet pipe diameter is used to indicate the inlet hydraulic diameter.

The formula for calculating the turbulence intensity is shown in Formula (11).

$$I = 0.16 \times Re^{-\frac{1}{8}} \tag{11}$$

In the formula: Re—The Reynolds number, and Re is calculated as in Formula (12);

$$Re = \frac{\rho \times v \times d}{\mu} \tag{12}$$

In the formula:

ρ—The density of the fluid, in kg/m^3;

V—The flow velocity of the fluid, in m/s;

μ—The viscosity coefficient of the fluid, in Pa*s,

d—A characteristic length, in m; When the fluid flows through a circular pipe, d is taken as the equivalent diameter of the pipe.

When the inlet pipe diameter is 0.2 m, the turbulence intensity of the medium chloroform in the pipe at each flow rate from 0.1 m/s to 1 m/s is shown in Table 4.

Table 4. Turbulence intensity of chloroform at each flow rate for a diameter of 0.2 m.

Flow Rate m/s	Turbulence Intensity %
0.1	4.0808
0.2	3.7412
0.3	3.5572
0.4	3.4315
0.5	3.3371
0.6	3.2619
0.7	3.1997
0.8	3.1467
0.9	3.1007
1.0	3.0602

2.4.3. Results of Numerical Simulation Calculations

The flow medium in the pipe is chloroform and the inlet flow velocity is 0.1 m/s–1 m/s. Therefore, the magnitude of the risk of erosion of the reducer is indicated by the magnitude of the wall shear stress, and the part shown in red is the area with the highest risk of erosion. In order to facilitate the representation, the reducer is unified with the following code: X-Y, where X is the outlet pipe diameter (mm) and Y is the inlet flow rate (m/s). For example, the outlet pipe diameter is 130 mm, and the inlet flow rate is 1.0 m/s, which is expressed as 130-1.0. Figure 11 shows the numerical simulation results of outlet pipe diameter 160 mm and flow rate 1.0 m/s, i.e., (160-1.0).

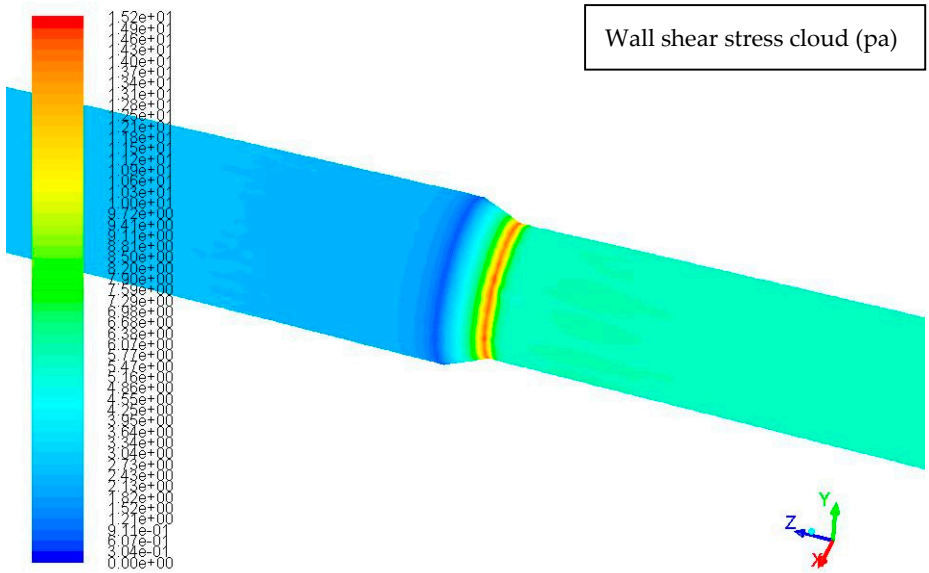

(**a**)

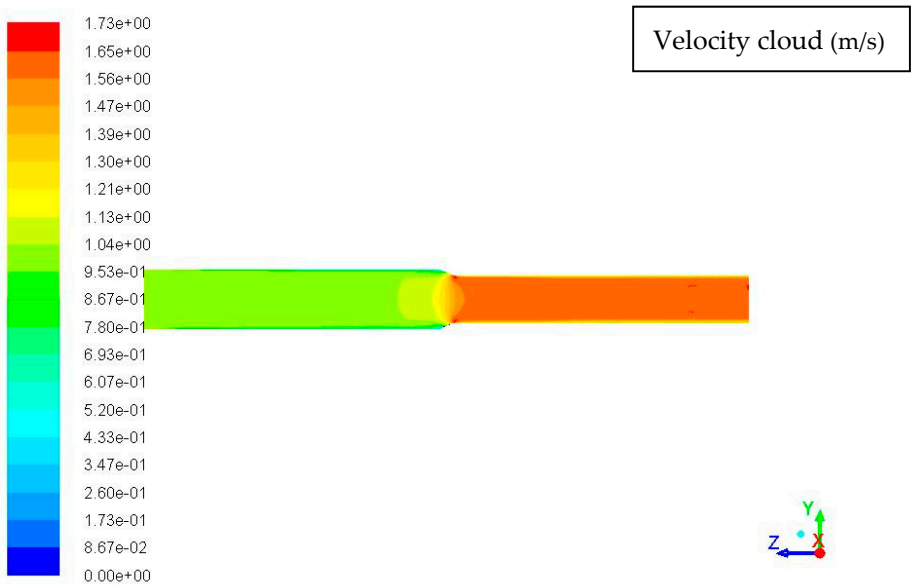

(**b**)

Figure 11. *Cont.*

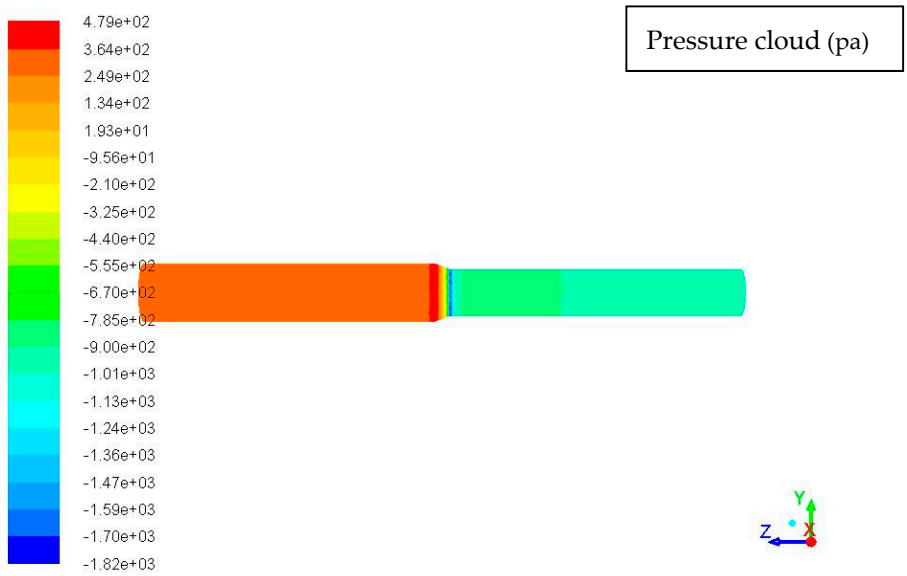

(**c**)

Figure 11. Numerical simulation results for outlet pipe diameter 130 mm and flow rate 0.1 m/s; (**a**) Wall shear stress cloud; (**b**) Velocity cloud; (**c**) Pressure cloud.

2.4.4. Analysis of the Results

According to the calculation results, the influence of flow rate on the erosion of reducer is plotted in Figure 12. Analysis shows that:

(1) when the outlet pipe diameter (taper) and other conditions do not change, with the increase in flow rate, the maximum wall shear stress and maximum pressure are increased;

(2) when the flow rate is constant, the maximum wall shear stress and pressure are reduced as the outlet diameter increases, i.e., the taper of the conical tube decreases;

(3) the larger the inlet flow rate, the greater the difference between the maximum wall shear stress and pressure corresponding to the different outlet pipe diameters of the reducer

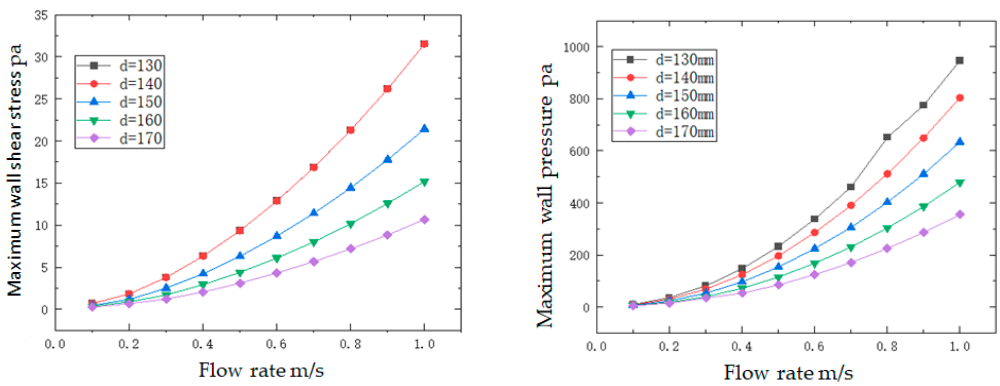

(**a**) (**b**)

Figure 12. The influence of flow rate on the erosion of the reducer; (**a**) Trend of maximum wall shear stress; (**b**) Trend of maximum wall pressure.

2.4.5. Prediction of Erosion-Prone Areas of the Reducer

(1) From the wall shear stress cloud, along the direction of fluid flow, wall shear stress in the inlet section of the pipe diameter decreases before the basic unchanged, and the value is small; when the pipe diameter decreases (the left side of the tapered tube),

wall shear stress and the size of the outlet pipe diameter is inversely proportional; when the pipe diameter decreases to the same diameter as the outlet pipe (the right end of the tapered tube), the wall shear stress at this location reaches its maximum value.

(2) From the velocity cloud, in the inlet section of the reducer, the velocity size is the minimum and basically constant throughout the process; when the fluid flows into the diameter change region, with the diameter of the pipe decreases, the velocity increases; when the fluid reaches the outlet section, the velocity increases to the maximum value, the velocity basically remains the same.

(3) From the pressure cloud, in the entrance section of the reducer, because the wall is not smooth, the fluid flow in the pipe needs to overcome friction resistance, so the size of the pressure in the direction of fluid flow gradually decreases; when the fluid reaches the pipe diameter reduction (the left end of the tapered pipe), according to Bernoulli's equation, with the reduction of the pipe diameter, the flow rate increases and the pressure decreases; in the outlet section of the pipe, the pressure again with the fluid flow; in the outlet section of the pipe, the pressure decreases with the direction of fluid flow.

In summary, the location of the reducer pipe with higher risk of erosion is located at the reduction of the pipe diameter, and the risk of erosion is greatest when the pipe diameter is reduced to the outlet pipe diameter location. In the case of constant pipe diameter and other conditions, the size of the reducer pipe erosion risk is proportional to the medium flow rate, and in the case of constant inlet flow rate, the size of the reducer pipe erosion risk is proportional to the outlet diameter of the reducer pipe and inversely proportional to the tapered pipe taper.

2.5. Prediction Study of Erosion-Prone Areas of the Tee

2.5.1. Modeling and Meshing

The same as the reducer, the GEOMETRY module is used to model the tee, and the MESH module is used to divide the tee model mesh. The structure diagram of the tee is shown in Figure 13, and the 3D model diagram of tee is shown in Figure 14

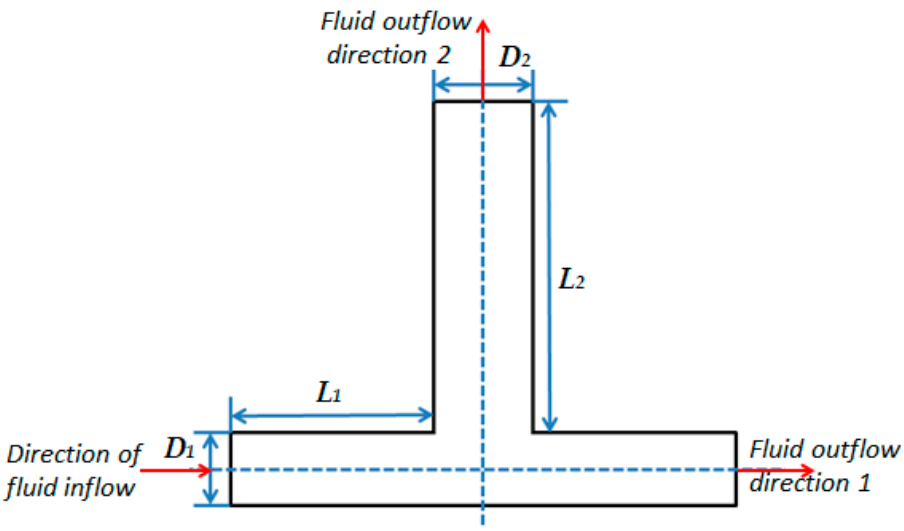

Figure 13. The model diagram of the tee.

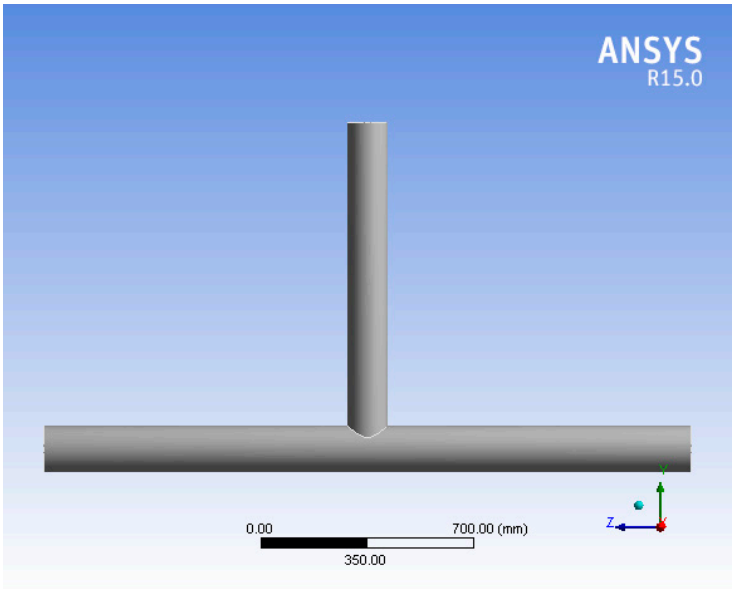

Figure 14. The 3D model diagram of the tee.

In Figure 13, D_1 end is the fluid inlet end, D_2 end and D_3 is the fluid outlet end, the direction shown by the arrow is the direction of fluid flow in the pipe and L_1 and L_2 are the pipe lengths of the reducer inlet and outlet pipes, respectively. In order to eliminate the influence of pipe import and export on the study results of the tee erosion, take $L_1 = L_2 = 1000$ mm. D_1 is the inlet diameter of the tee; D_2 is the outlet diameter of the tee tube in vertical direction; the outlet diameter of outlet 1 is kept constant with D_1, and the influence of the change of outlet diameter on erosion is studied by changing the outlet diameter D_2 of outlet 2.

Similarly, the mesh division of the tee is similar to that of the reducer, and the shape of the mesh division is chosen to be triangular. The number of boundary layers is 10, the incremental index is 1.2 and the maximum mesh width is 6 mm. The mesh division of the tee is shown in Figure 15.

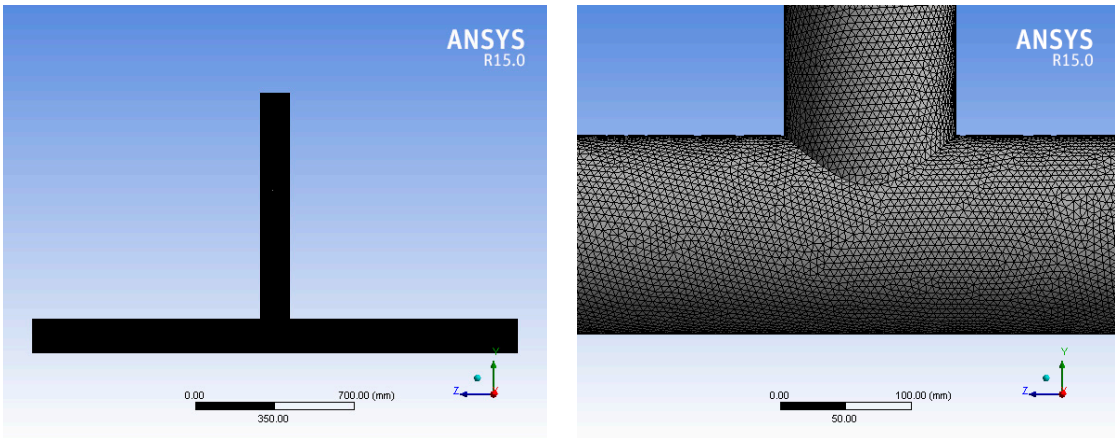

(**a**) (**b**)

Figure 15. The mashing result; (**a**) Overall view; (**b**) Partial view.

2.5.2. Boundary Condition Setting

The same as the reducer, the tee uses chloroform single medium as the flow medium in the pipe, and considering the influence of gravity, the gravity direction along the Y-axis direction and the gravity size are taken as -9.81 m/s^2. The density of chloroform is taken

as 1480 kg/m^3, the viscosity is taken as 0.00053 Pa*s and the inlet pressure is taken as 106 Pa. The medium parameters of the tee are shown in Table 3.

According to the actual situation, the low flow rate of 0.1 m/s, 0.2 m/s, 0.3 m/s, 0.4 m/s, 0.5 m/s, 0.6 m/s, 0.7 m/s, 0.8 m/s, 0.9 m/s, 1 m/s is taken to study the effect of flow rate on erosion; the inlet pipe diameter and the outlet pipe diameter of outlet 1 are taken to be 150 mm, and the pipe diameters of vertical pipe (D_2) are: 150 mm, 140 mm, 130 mm, 120 mm, 110 mm, so as to change the ratio of inlet and outlet pipe diameters of the tee pipe on erosion. 140 mm, 130 mm, 120 mm, 110 mm, so as to change the ratio of the inlet and outlet of the tee pipe and study the influence of the inlet and outlet pipe diameter ratio on the erosion.

The same as the reducer, the turbulence intensity of the medium chloroform in the tube at each flow rate from 0.1 m/s to 1 m/s for an inlet diameter of 150 mm is shown in Table 5.

Table 5. Turbulence intensity of chloroform at each flow rate for a diameter of 0.15 m.

Flow Rate m/s	Turbulence Intensity %
0.1	4.2302
0.2	3.8791
0.3	3.6874
0.4	3.5572
0.5	3.4593
0.6	3.3814
0.7	3.3168
0.8	3.2619
0.9	3.2143
1.0	3.1722

2.5.3. Results of Numerical Simulation Calculations

The magnitude of the erosion risk of the tee is indicated by the magnitude of the wall shear stress, with the highest erosion risk shown in red. For the convenience of representation, the tee is uniformly expressed by the following code: X-Y, where X is the outlet 2 (D_2) pipe diameter (mm), and Y is the inlet flow rate (m/s). For example: outlet 2 (D_2) pipe diameter of 130 mm, inlet flow rate of 1.0 m/s, expressed as 130-1.0. 110-1.0 tee tube numerical simulation results are shown in Figure 16.

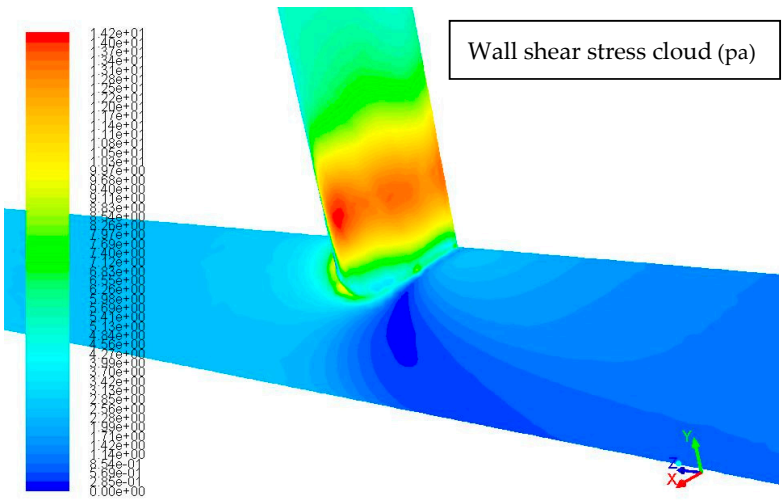

(**a**)

Figure 16. *Cont.*

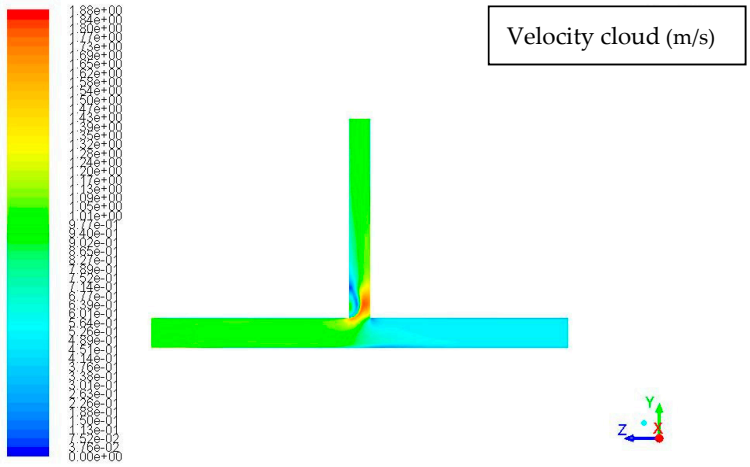

(**b**)

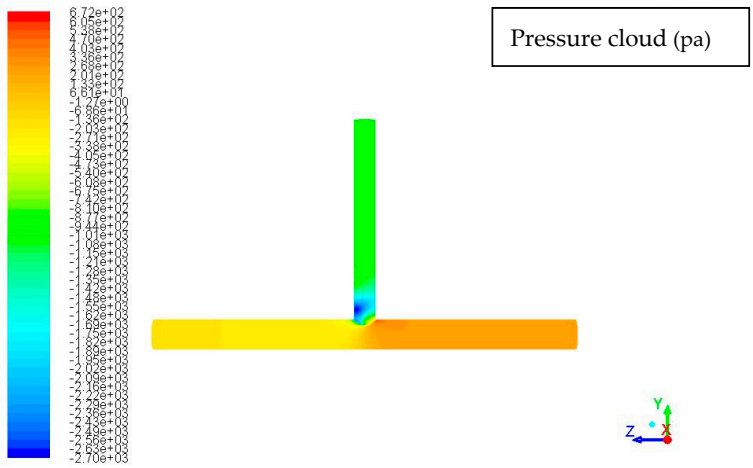

(**c**)

Figure 16. Numerical simulation results for the tee outlet pipe diameter 110 mm, flow rate 0.1 m/s; (**a**) Wall shear stress cloud; (**b**) Velocity cloud; (**c**) Pressure cloud.

2.5.4. Analysis of the Results

According to the calculation results, the influence of flow rate on the erosion of the tee is plotted in Figure 17. Analysis shows that:

(1) The size of the maximum wall shear stress under each pipe diameter is proportional to the flow rate, the wall shear stress growth rate is proportional to the flow rate; that is, with the increase in medium flow rate, the risk of erosion of the tee pipe is also increased.

(2) Comparing the magnitude of wall shear stress of different pipe diameters under any flow, it can be obtained that the vertical outlet pipe diameter of the tee pipe is inversely proportional to the maximum wall shear stress; that is, the risk of erosion of the tee pipe is subsequently reduced.

(3) With the increase in flow rate, the difference in the size of the maximum wall shear stress of different pipe diameters is also greater; that is, the greater the flow rate, the more obvious the effect of pipe diameter on the risk of erosion.

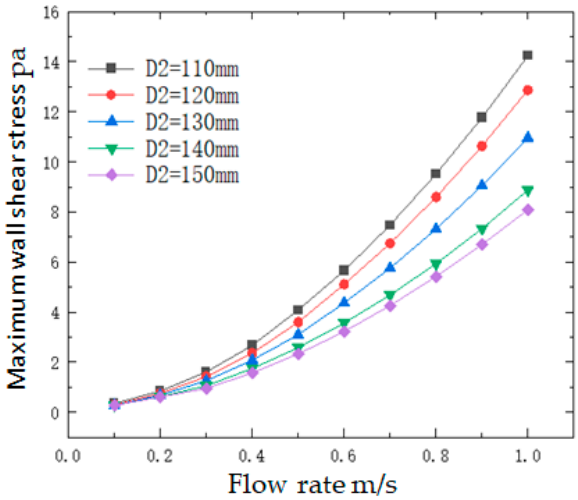

Figure 17. The influence of flow rate on the erosion of the tee.

2.5.5. Prediction of Erosion-Prone Areas of the Tee

(1) Horizontal direction, the inlet pipe section direction of wall shear stress with the direction of fluid flow gradually decreases. The tee pipe branch, near the entrance side of the horizontal pipe and vertical pipe junction wall shear stress increased significantly; located in the vertical outlet of the tee pipe near the horizontal outlet side of the tee pipe wall shear stress is the largest position, after the maximum wall shear stress position, along the vertical branch fluid flow direction, wall shear stress is gradually reduced; horizontal wall shear stress in the direction of fluid flow gradually reduced.

(2) From the velocity cloud, we can get that the velocity of the inlet pipe section remains basically unchanged, and the flow velocity increases where the wall shear stress increases, and the velocity reaches the maximum in the area of the vertical branch pipe near the horizontal direction side, which is the same as the wall shear stress position.

(3) From the pressure cloud, the pressure throughout the inlet section of the pipe is basically constant. In the direction of the vertical vertical branch pipe, the pressure reaches a minimum value at the position of maximum velocity. After this position, the pressure increases in the direction of vertical pipe fluid flow, increases to a certain value and then remains unchanged; in the direction of the horizontal branch pipe, the pressure increases at the intersection of the three pipes, increases to a certain value and then remains unchanged.

In summary: the tee erosion risk is the largest area is located in the vertical branch pipe against the horizontal branch pipe outlet side; pipe diameter and other conditions remain unchanged, the tee pipe erosion risk increases with the increase in media flow rate; inlet flow rate and other parameters remain unchanged, the tee erosion risk decreases with the vertical outlet diameter of the tee pipe; the larger the inlet flow rate, the greater the risk of erosion.

2.6. Prediction Study of Erosion-Prone Areas of the Valve

2.6.1. Modeling and Meshing

As above, GEOMETRY is used to establish the geometric model of the bend pipe. The bend pipe diameter D is designed as 80 mm, 100 mm, 125 m, 150 mm, 175 mm; valve inlet pipe length $L_1 = 5D$, outlet pipe length $L_3 = 5D$; gate valve width L_2 is known according to the wedge gate thickness dimension, when the pipe diameter is 80 mm L_2 = 47.5 mm, when the pipe diameter is 100 mm L_2 = 52.5 mm, when the pipe diameter is 125 mm L_2 = 55.5 mm, L_2 = 67.5 mm when the pipe diameter is between 150~200 mm; the valve opening of pipe diameter 80 mm is set to 0.25, 0.5, 0.75, and the valve opening of other pipe diameters is set

to 0.5. The model diagram of the valve is shown in Figure 18. The 3D model diagram of the valve is shown in Figure 19. Table 6 shows the valve specification design table.

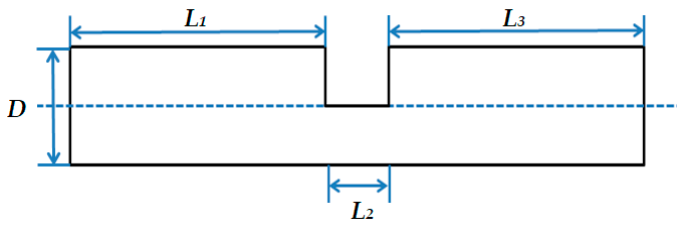

Figure 18. The model diagram of the valve.

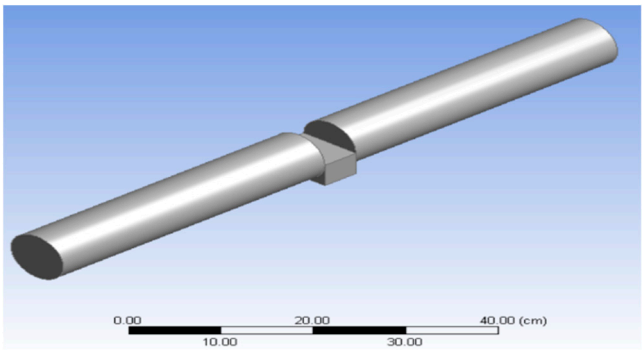

Figure 19. 3D model diagram of the valve.

Table 6. Valve specification design table.

Valve Number	Valve Opening	D mm	L_1 mm	L_2 mm	L_3 mm
1	0.25	80	400	47.5	400
2	0.5	80	400	47.5	400
3	0.75	80	400	47.5	400
4	0.5	100	500	52.5	500
5	0.5	125	625	55.5	625
6	0.5	150	750	67.5	750
7	0.5	175	875	67.5	875

MESH function is applied for meshing, and the number of meshes is 1 million. The mesh division is done by the block method, especially refining the mesh of the wall, which is the focus of the numerical simulation, to reduce the calculation volume of other non-focused calculation areas and shorten the calculation period while ensuring the calculation accuracy of the calculation area. The mesh division of the tee is shown in Figure 20.

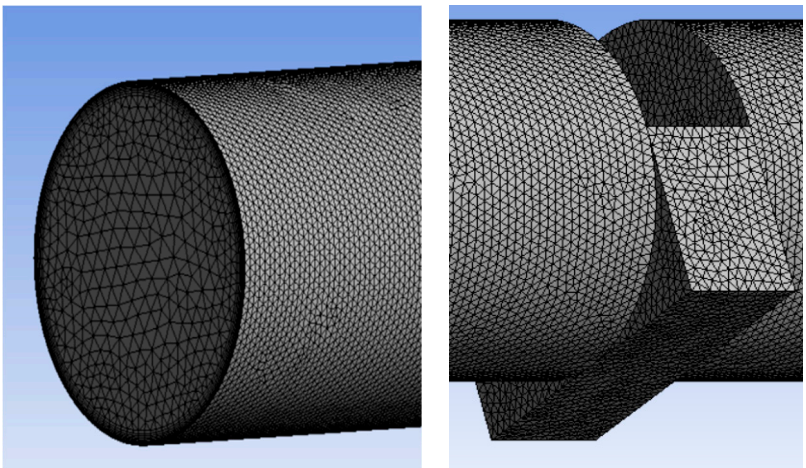

(**a**) (**b**)

Figure 20. The mashing result; (**a**) Partial view; (**b**) Partial view.

2.6.2. Boundary Condition Setting

The same as the reducer, the tee uses chloroform single medium as the flow medium in the pipe, considering the influence of gravity, the gravity direction along the Y-axis direction and the gravity size taken as -9.81 m/s^2. The density of chloroform is taken as 1480 kg/m^3, the viscosity is taken as 0.00053 Pa*s and the inlet pressure is taken as 106 Pa. The medium parameters of the tee are shown in Table 3.

Since the inlet flow velocity of the valve is known, the inlet boundary condition uses the inlet velocity. The inlet velocity range is 0.1 m/s~0.6 m/s, so the inlet velocity is set to 0.1 m/s, 0.2 m/s, 0.3 m/s, 0.4 m/s, 0.5 m/s, 0.6 m/s; the inlet pressure is 1,000,000 Pa; Table 7 is the valve inlet condition parameter table, set the pipeline outlet close to the fully developed situation, so the pipeline outlet chooses free flow outlet (outflow).

Table 7. Valve inlet conditions parameters table.

Flow Rate m/s	Turbulence Intensity %
0.1	4.5759
0.2	4.1962
0.3	3.9888
0.4	3.8479
0.5	3.7420
0.6	3.6577

2.6.3. Results of Numerical Simulation Calculations

As the medium used is chloroform single-phase flow, the size of the risk of scour corrosion of the reducer is indicated by the size of the wall shear stress, and the part shown in red is the area with the highest risk of scour corrosion. In order to facilitate the representation, the cloud is unified using the following code: numbering using the valve + pipe diameter + flow rate form. For example: valve for 0.25, pipe diameter of 80 mm, inlet flow rate of 0.1 m/s, the number is 2,508,001. Figure 21 for (2,508,001) valve for 0.25, pipe diameter of 80 mm, inlet flow rate of 0.1 m/s simulation of the cloud.

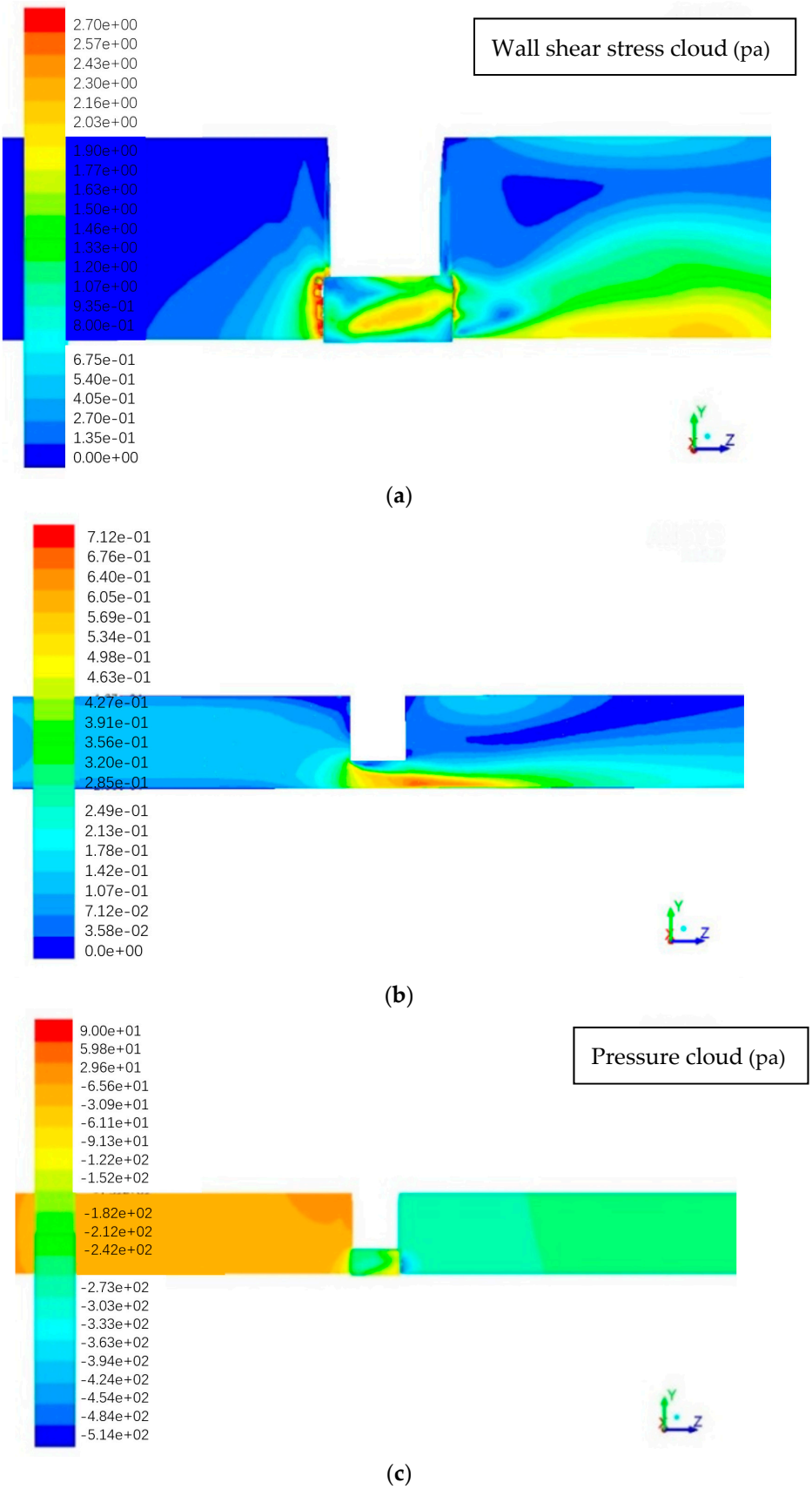

Figure 21. Numerical simulation results for the tee outlet pipe diameter 110 mm, flow rate 0.1 m/s; (**a**) Wall shear stress cloud Figure; (**b**) Velocity cloud; (**c**) Pressure cloud.

2.6.4. Analysis of the Results

(1) According to the calculation results, the influence of flow rate on valve erosion is shown in Figure 22. Analysis shows that: when the valve specifications remain unchanged, with the increase in fluid flow rate in the valve, the valve is subjected to the maximum pressure exponentially increased, the valve is subjected to the maximum pressure of the static pressure of the liquid and the sum of the pressure of the valve itself; according to the Formula (13), the fluid kinetic energy with the fluid flow rate is exponentially increased, so the pressure at this location is also exponentially increased with the flow rate. Valve shear stress with the increase in flow rate, wall shear stress and unit element velocity perpendicular direction of the flow rate change rate increases, so the valve is subjected to increased wall shear stress.

$$\tau = \mu \frac{dv}{dy} \tag{13}$$

In the formula:
τ—the wall shear stress. In N;
μ—The fluid viscosity;
dv—The flow velocity on unit element. In m/s;
dy—The width of flow velocity variation on unit element. In m.

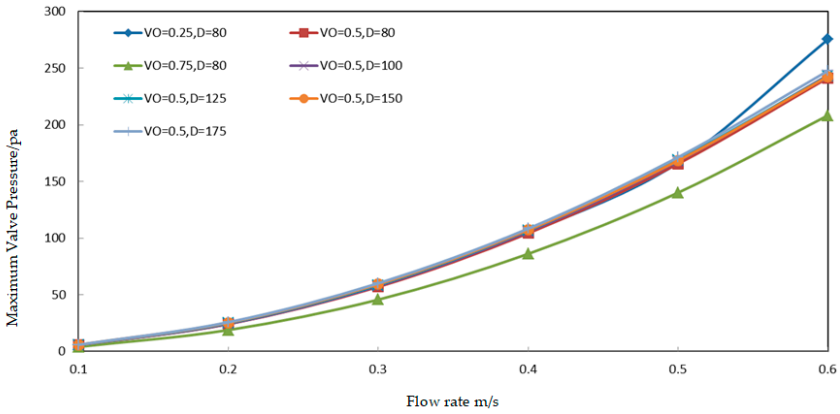

(**a**)

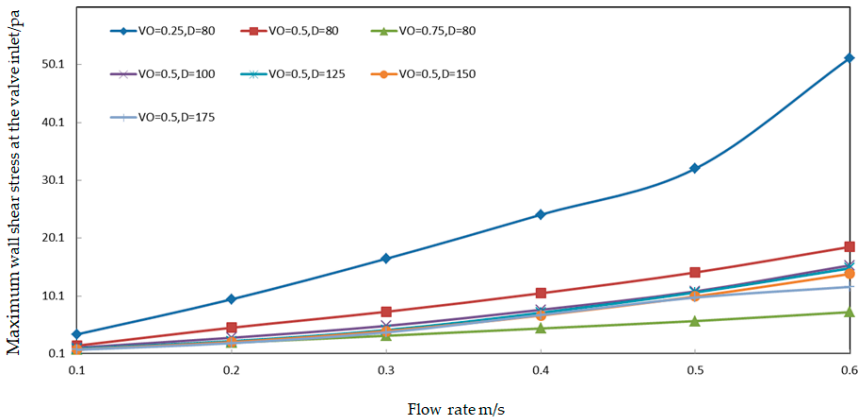

(**b**)

Figure 22. *Cont.*

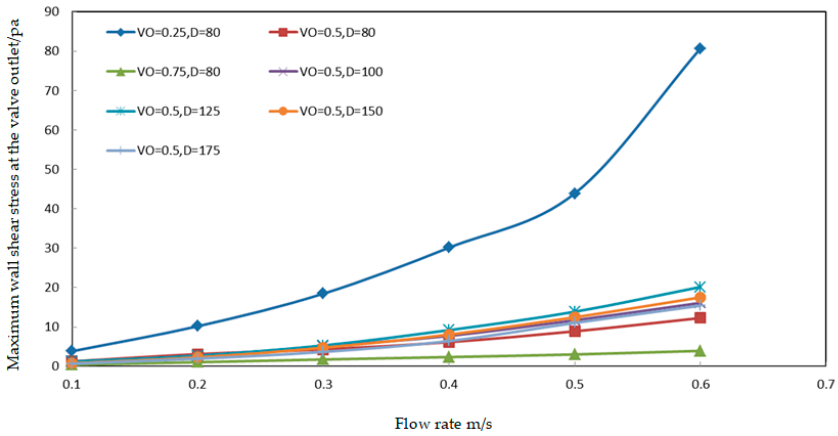

(**c**)

Figure 22. The influence of flow rate on the erosion of the valve; (**a**) Trend of maximum wall pressure; (**b**) Trend of maximum wall shear stress at the valve inlet; (**c**) Trend of maximum wall shear stress at the valve outlet.

(2) The influence of pipe diameter on valve erosion is shown in Figure 23. When the valve opens, flow rate and other conditions remain unchanged and the maximum pressure on the valve increases slightly with the increase in pipe diameter; the maximum wall shear stress at the gate valve inlet increases with the increase in pipe diameter; the wall shear stress near the outlet of the gate valve increases with the increase in pipe diameter and reaches a peak near the wall shear stress when the pipe diameter reaches about 125 mm and then decreases with the increase in pipe diameter.

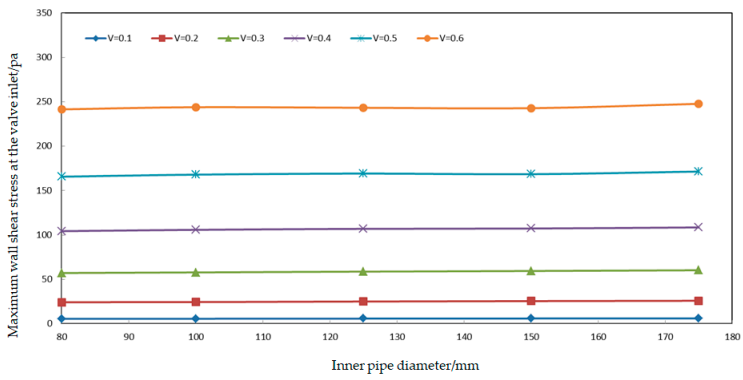

(**a**)

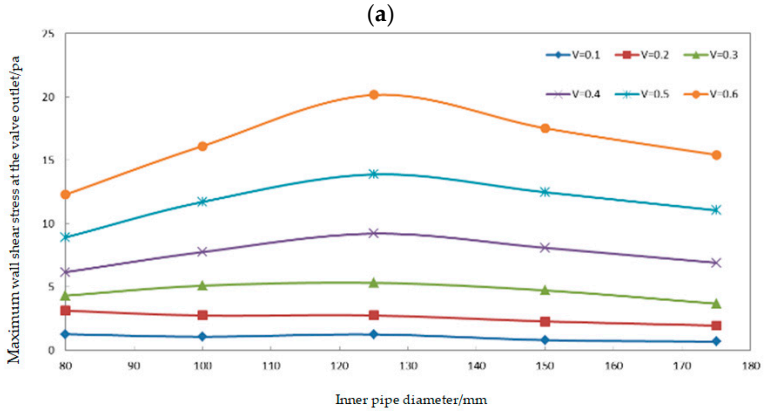

(**b**)

Figure 23. The influence of inner pipe on the erosion of the valve; (**a**) Trend of maximum wall shear stress at the valve inlet; (**b**) Trend of maximum wall shear stress at the valve outlet.

(3) The influence of valve opening on valve erosion is shown in Figure 24. When the valve flow rate, pipe diameter and other factors remain unchanged, the maximum pressure on the valve decreases with the increase in opening; the wall shear stress on the valve decreases sharply with the increase in opening. The opening of the valve increases, the cross-sectional area available for fluid passage increases, the flow pattern in the tube tends to flatten, the pressure distribution of the valve itself is uniform, so the maximum pressure on the valve is reduced. Valve opening increases, the fluid passed at the gate valve slows down, the flow rate decreases, the boundary layer at some locations increases, and the valve is subjected to a sharp decrease in wall shear stress under the joint action of both.

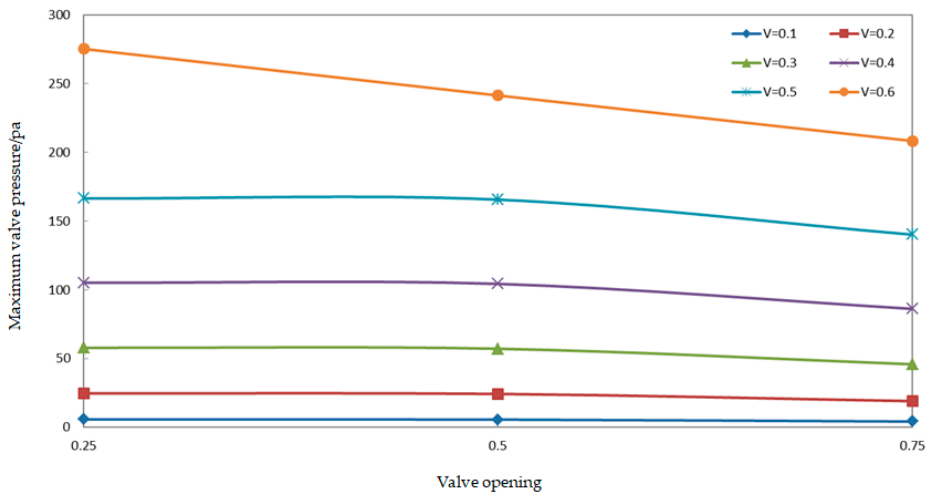

(**a**)

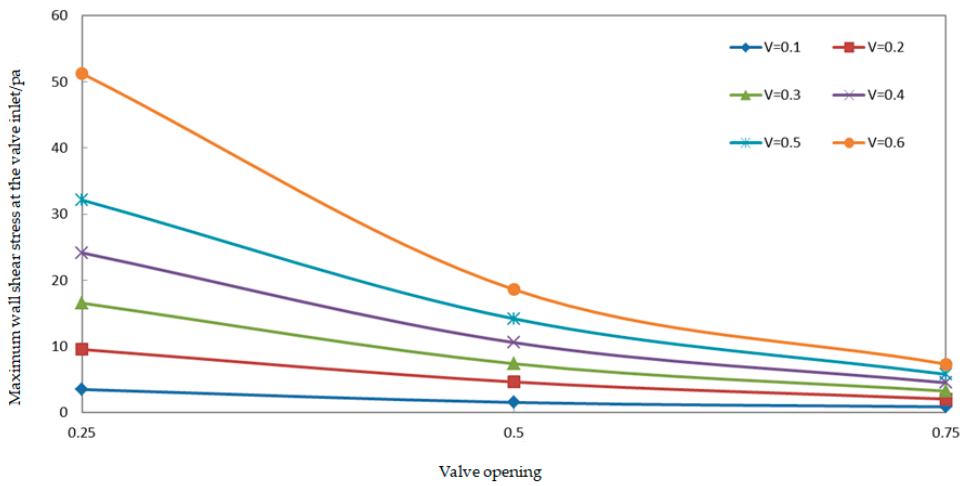

(**b**)

Figure 24. *Cont.*

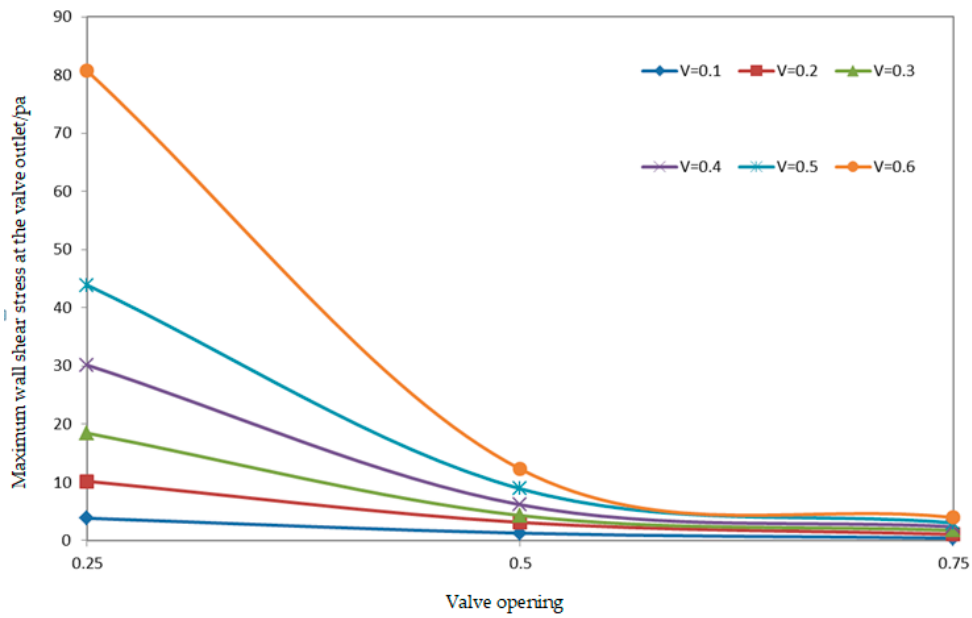

(**c**)

Figure 24. The influence of valve opening on the erosion of the valve; (**a**) Trend of maximum wall pressure; (**b**) Trend of maximum wall shear stress at the valve inlet; (**c**) Trend of maximum wall shear stress at the valve outlet.

2.6.5. Prediction of Erosion-Prone Areas of the Tee

According to the above numerical simulation data, through collation and analysis, the effect of valve flow rate, pipe diameter, opening degree on the valve erosion.

(1) When the valve flow rate, pipe diameter and other factors remain unchanged, the maximum pressure on the valve decreases with the increase in the opening degree; the wall shear stress on the valve decreases sharply with the increase in the opening degree.
(2) Analysis of pressure changes, the valve opening increases, the cross-sectional area available for fluid through the increase, the flow pattern tends to flatten, the valve itself, the pressure distribution, so the maximum pressure under the valve is reduced.
(3) Analysis of the change in shear stress, the opening increases, the fluid passing at the gate valve slows down, the flow rate decreases, the boundary layer at some locations increases, and the valve is subjected to a sharp decrease in wall shear stress under the combined effect of both.

3. Database Establishment Method

The database system is developed in C# language and ASP.NET, and requires data server, web server and client to run. It includes four modules: basic data management, pipeline erosion legend, pipeline GIS platform and system background management.

Basic data management includes pipeline basic data management and container basic data management; pipeline erosion legend includes pipeline erosion legend management and pipeline erosion legend retrieval; pipeline GIS platform includes pipeline 2D and 3D graphic information display and process-based pipeline erosion retrieval.

The database system adopts a three-layer architecture to divide the whole business application into: presentation layer (UI), business logic layer (BLL) and data access layer (DAL). In terms of architecture, advanced B/S (browser/server) structure is used. C# language and ASP.NET development tools are used.

GIS-based functional display platform. The system takes advantage of the computer graphics technology of intuitive expression of GIS map and superimposes the equipment process flow map on the basic GIS topographic map. Through the GIS mode functional

platform, system users can intuitively and easily find and locate the location of pipelines and erosion parts of pipelines, and display pipeline and erosion data in the form of text, thematic classification and statistical chart expression through the input and output interfaces provided by the map window [24].

3.1. System Characteristics

In the structure, the advanced B/S (browser/server) structure is adopted, which has the characteristics of distributed business processing such as querying and browsing any time and at any place. With easy and convenient business expansion, server functions can be increased by adding pages; easy maintenance, strong sharing, etc.

The database interface is based on a paper-based low-fidelity prototype (Paper Prototype) that can be tested and improved by users. In structural design, the logical classification of the directory system and the definition of words is an important prerequisite for comprehension and operation by users.

3.2. System Functions

The system construction is divided into four layers: basic data management layer, pipeline scour and corrosion legend layer, pipeline GIS platform layer and system background management.

(1) Basic data management layer: the interface between basic data management layer and ERP system can update the basic information of pipeline and vessel according to the ERP information according to the equipment number. It can also read ERP related information into EXCEL table according to equipment number for further processing. The basic data management layer supports data import in the form of EXCEL tables or, if the ERP system provides a Web Service interface, the necessary ERP file data can be imported into the file database, avoiding duplicate data input and improving work efficiency.

(2) Pipeline scouring corrosion parts legend database layer: the content includes typical pipe fittings based on the flow field analysis of the scouring corrosion parts diagram, covering different structural characteristics of the pipe model, the database diagram example Figure 25.

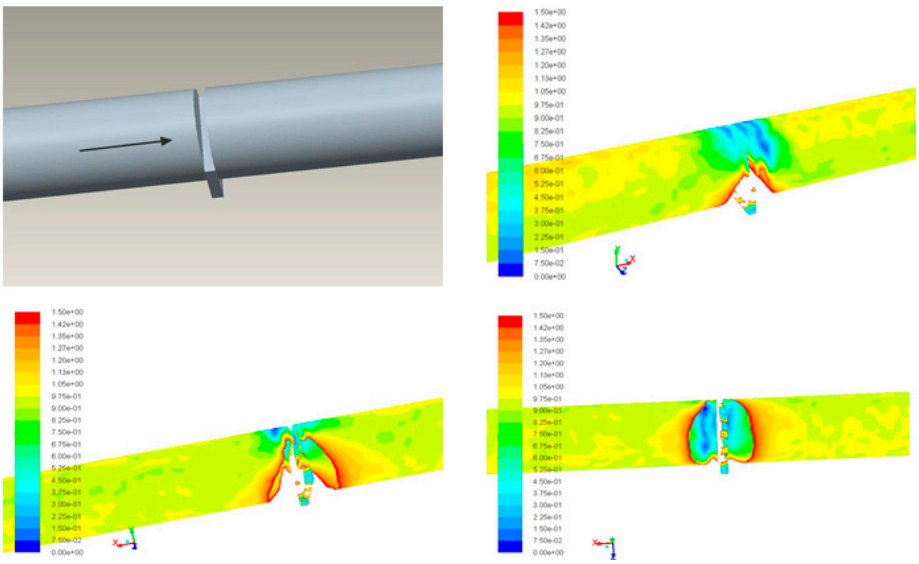

Figure 25. Legend in the database.

(3) Pipeline scouring corrosion GIS platform layer: users can browse the PFD diagram of the relevant device through the system and can carry out the basic browsing operation of the diagram + m. Users can also quickly locate the easy and pipeline in the device

diagram by pulling the box with the mouse, and the system will query the relevant information of the function and pipeline according to the current function status.

(4) System background management: Three role types are used, including system administrator, branch administrator and non-administrator. Users without role type have different authority to realize the secondary management of main plant and branch plant.

4. Case Application

The method has been more widely and deeply applied in some large refining companies in China, overseas oil fields and other enterprises for demonstration. In this paper, an application demonstration case is selected to analyze the scour corrosion of distillation oil and gas line, distillation II middle line and hydrogenation combined unit reactant line of a large oil and gas enterprise in western China. The following is the practical application of the method to distillate oil and gas lines 01-EA002/1 and 01-EA002/2 of a large oil and gas enterprise in western China.

4.1. Case Overview

Distillate 01-EA002/1 and 01-EA002/2 of a large oil and gas company in western China were eroding severely during operation. The pipe fitting parameters are shown in Tables 8 and 9. The structure diagram is shown in Figure 26.

Table 8. The parameters of the pipe fittings of 01-EA002/1.

Name of chemical plant	I distillation gasoline line	Pipe name	Gasoline line
Pipe number	01-EA002/1	Pipeline level	GC2
starting point	C-1001	End position	E-1001/1-4
Work pressure	0.13	Operating temperature	100
Working medium	gasoline	Pipe material	20#
Pipe specification (Outer diameter mm × Wall thickness mm)		φ630 × 12	

Table 9. The parameters of the pipe fittings of 01-EA002/2.

Name of chemical plant	I distillation gasoline line	Pipe name	Gasoline line
Pipe number	01-EA002/2	Pipeline level	GC2
starting point	E-1001/1-4	End position	E-1001/1-4
Work pressure	0.11	Operating temperature	80
Working medium	gasoline	Pipe material	20#
Pipe specification (Outer diameter mm × Wall thickness mm)		φ426 × 0.95/φ273 × 8.5	

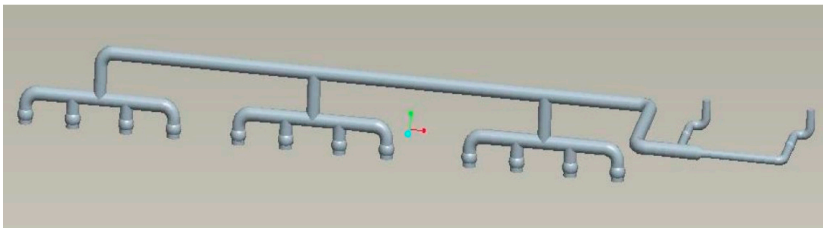

(**a**)

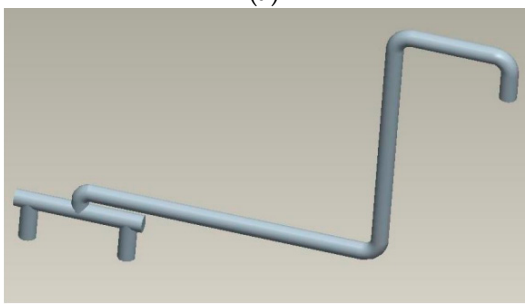

(**b**)

Figure 26. The 3D structure diagram of pipelines, (**a**) The 3D structure diagram of a 01-EA002/1; (**b**) The 3D structure diagram of a 01-EA002/2.

4.2. Numerical Simulation

Pipeline 01-EA002/1 uses the steady-state two-phase flow coupling method, and pipeline 01-EA002/2 uses the steady-state two-phase flow discrete method to reduce the calculation time. The parameters of the pipe fittings are shown in Tables 8 and 9.

4.3. Prediction of Erosion-Prone Areas of Pipeline 01-EA002/1

The erosion distribution of pipeline 01-EA002/1 based on impact velocity is shown in Figure 27, the magnitude of which can be found in the color of the legend.

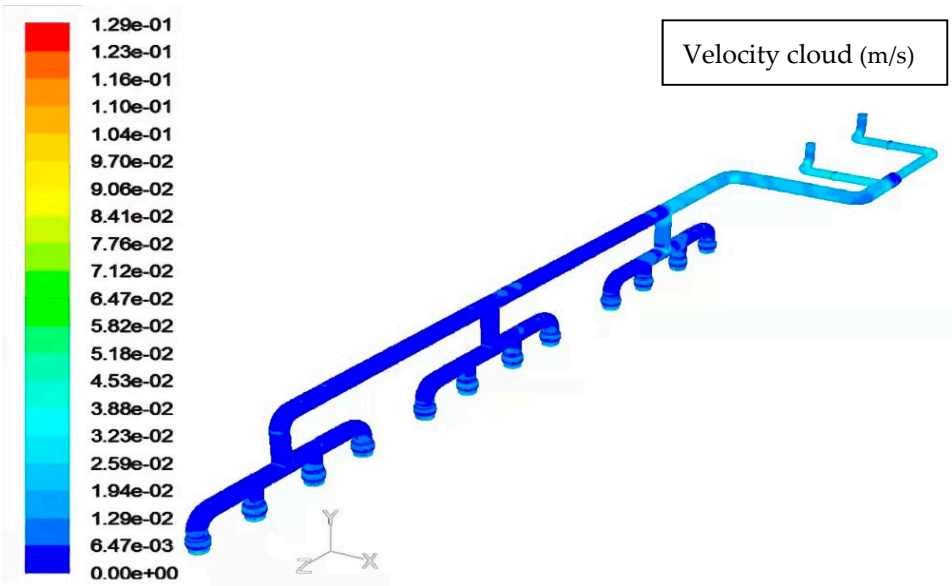

(**a**)

Figure 27. *Cont.*

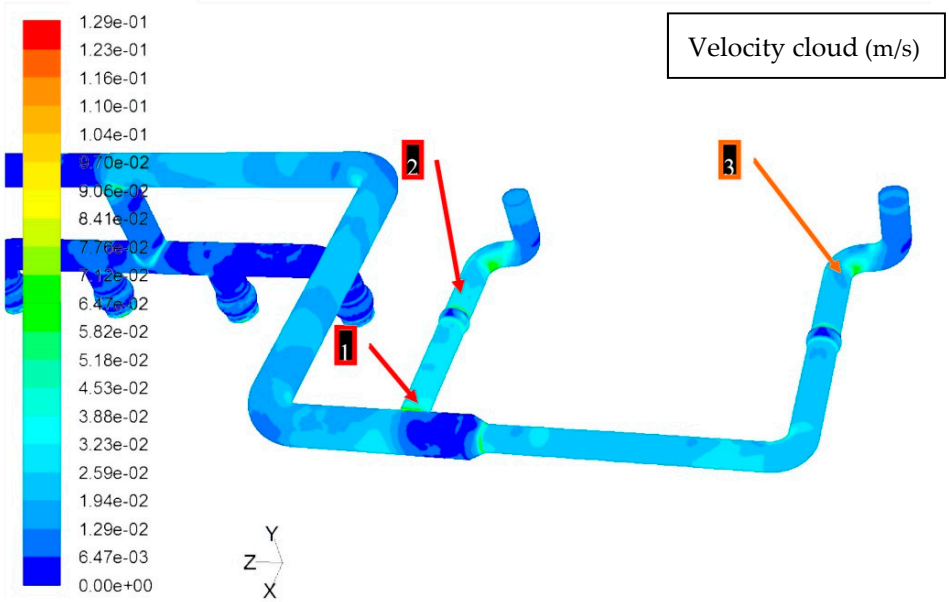

(**b**)

Figure 27. The erosion distribution map of pipeline 01-EA002/1, (**a**) General view of erosion division; (**b**) Partial view of erosion division.

01-EA002/1 has only one specification φ 630 × 12, according to the principle of discriminating factors affecting the predicted results of scouring corrosion parts, scouring corrosion thinning area shown in Figure 27b, of which 1 is the most dangerous area, 2, 3 (inside and outside of the elbow, it is recommended to test the whole elbow) is the second most dangerous area, it is recommended that inspectors do a detailed inspection in this area.

4.4. Prediction of Erosion-Prone Areas of Pipeline 01-EA002/1

Pipeline 01-EA002/2. Based on the impact velocity of the scouring corrosion distribution in Figure 28; the size of the volume can be referred to the legend color; the spherical part of the figure indicates the fully open state of the gate valve flow channel. In 01-EA002/2, there are two pipe specifications φ 426 × 9.5 and φ 273 × 8.5 because the wall thickness of the pipe part of the scour corrosion effect is smaller, so do not consider the impact of different specifications. According to the prediction of scouring corrosion parts to discriminate factors, scouring corrosion thinning area from Figure 28b shown, of which, 1 (tee branch), 2 (elbow outlet to the gate valve) is the most dangerous area, 3 (elbow outlet to the gate valve) is the next dangerous area; it is recommended that inspectors in this area do a detailed inspection.

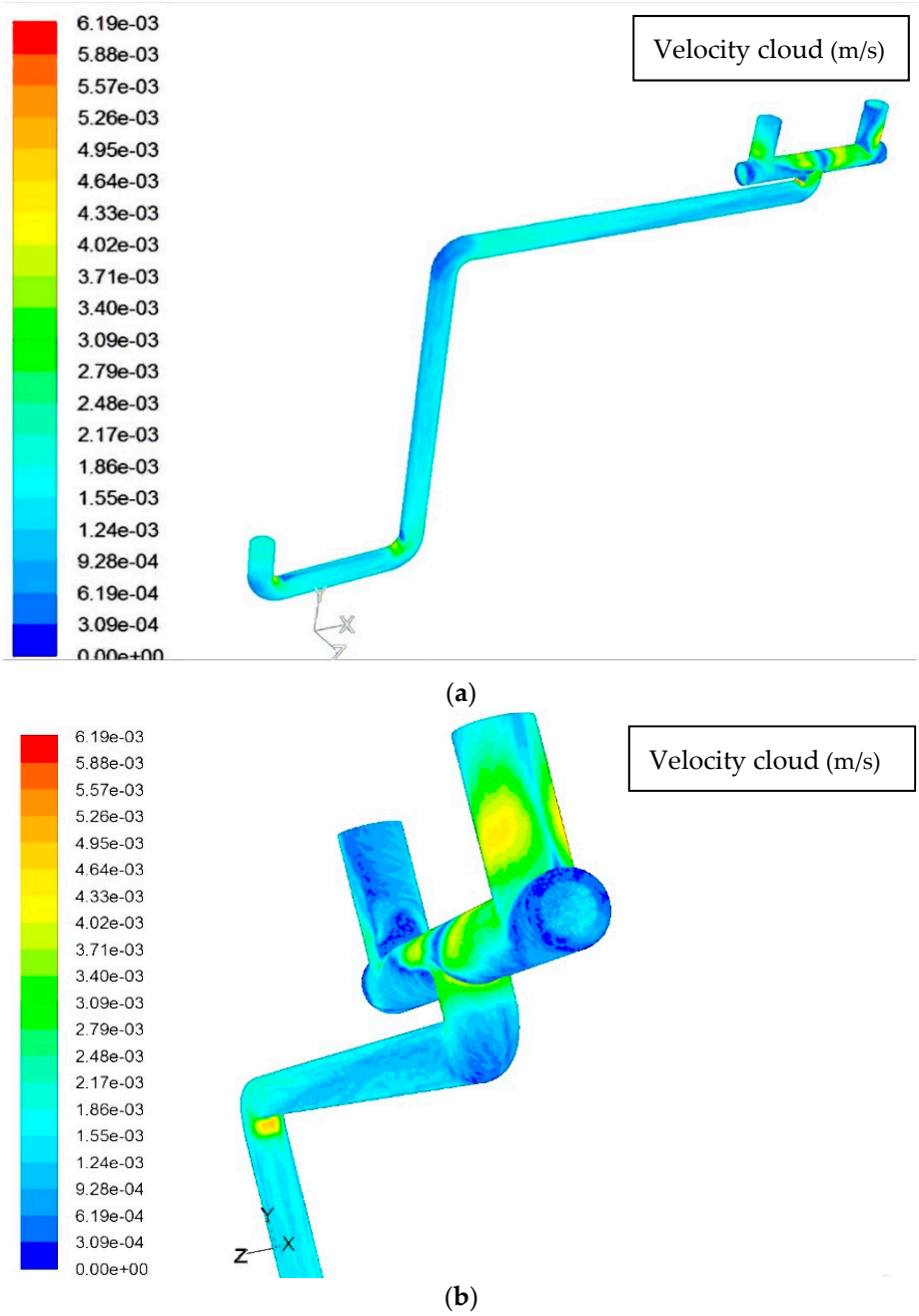

Figure 28. The erosion distribution map of pipeline 01-EA002/2, (**a**) General view of erosion division; (**b**) Partial view of erosion division.

4.5. Database Establishment

Compare the condition of erosion parts with similar data in the previous database. If the conditions are consistent, they are imported into the database. If they do not match, a regression operation is performed on both.

The database can be checked, maintained and enriched at a later stage using acoustic emission techniques. The pipeline erosion parts prediction method to be studied by the project forms a complete closed-loop technical route for scientific research by combining theoretical research, experimental device development, numerical simulation research, and field application demonstration; through the implementation of the project, a number of experimental platforms, computational models, test methods, data results, application demonstration methods and other achievements with independent intellectual property

rights are accumulated; to achieve scientific, reasonable and economic prediction of pipeline prone to erosion part, for online erosion monitoring to provide a direct and effective monitoring deployment planning map. Fang Zhou et al.'s research ideas also provide ideas for information management data technology [24–26].

5. Conclusions

In this paper, by summarizing the working conditions of fluorine chemical industry and the factors affecting pipe erosion, the three-dimensional flow field of three kinds of pipe fittings, such as tees, reducers and valves, under various fluorine chemical industry working conditions, was numerically calculated using the standard K-ε model with chloroform as the single-phase flow medium. The pressure and pipe wall shear stresses under different medium flow rates and pipe geometries were calculated to reveal the influence law of various factors on the erosion behavior of pipes. A database of pipe erosion legends for each pipe under common working conditions of fluorine chemical pipelines was established, covering 184 types of pipe erosion legends (including flow velocity, pressure and wall shear stress distribution clouds). Finally, the application of the method in a distillation oil and gas line of a large oil and gas enterprise in western China is described in detail.

Author Contributions: Writing—original draft preparation, Z.F.; Conceptualization, P.S. and J.Y.; writing—review and editing, C.S.; software, J.F. and J.D. All authors have read and agreed to the published version of the manuscript.

Funding: This research was funded by 2020YFB1506105/BUCTRC202026.

Institutional Review Board Statement: Not applicable.

Informed Consent Statement: Not applicable.

Data Availability Statement: The data presented in this study are available in the chart in this paper.

Acknowledgments: This paper is based on the national key special projects "Research on performance detection and quality evaluation technology of high pressure and large capacity hydrogen storage bottle (2020YFB1506105)" and "The talent introduction project of Beijing University of Chemical Technology (BUCTRC202026)" Thanks for the help and support of these project funds.

Conflicts of Interest: The authors declare no conflict of interest.

References

1. Chen, M.G. Fireball modeling and thermal hazards analysis of leaked 1,1-difluoroethane in fluorine chemical industry based on FDS. *Therm. Anal. Calorim.* **2020**, *146*, 1–12. [CrossRef]
2. Yao, Q.; Diao, J. Resource utilization of "three wastes" in fluorine chemical industry. *Environ. Prot. Chem. Ind.* **2017**, *37*, 289–293.
3. Guo, T.; Wu, J. State-dependent numerical simulation study of the reactive distillation process of 1-chloro-1,1-difluoroethane. *Chem. React. Eng. Processes* **2004**, *20*, 205–207.
4. Zeng, L.; Zhang, G.A.; Guo, X.P. Erosion–corrosion at different locations of X65 carbon steel elbow. *Corros. Sci.* **2014**, *85*, 318–330. [CrossRef]
5. Launder, B.E.; Spalding, D.B. *The Numerical Computation of Turbulent Flows*; Elsevier Sequoia, S.A.: Amsterdam, The Netherlands, 1990.
6. Zhao, M.Q. Principle and application of electrochemical method for determining corrosion rate of metals. *Chem. Clean.* **1992**, *8*, 1–5.
7. Li, C.H.F.; Zhang, Y.; Wang, B. Electrochemical study on CO_2 corrosion of X56 steel oil and gas gathering pipeline. *Nat. Gas Ind.* **2004**, *24*, 145–147.
8. Ahammed, M. Probabilistic Estimation of Remaining Life of a Pipeline in the Presence of Active Corrosion Defects. *Press. Vessel. Pip.* **1998**, *75*, 321–329. [CrossRef]
9. Wang, L.; Li, F. Probabilistic statistical analysis of pitting data of buried steel gas pipelines. *Gas Heat* **2004**, *24*, 657–659.
10. Li, T.J.; An, W.G. Reliability analysis of corroded pipes based on artificial neural network. *Mech. Eng.* **2005**, *6*, 106–107.
11. Xie, Y.; Yuan, Z.M. Application of gray dynamic model in predicting corrosion of gas transmission pipelines. *J. Southwest Pet. Inst.* **1999**, *21*, 50–51.
12. Su, X.; Yuan, Z.M. Corrosion prediction of gas pipeline based on "series grey prediction". *J. Southwest Pet. Inst.* **2006**, *28*, 82–83.
13. Jones, D.; Dawson, J. Risk Assessment Approach to Pipeline Life Management. *Pipes Pipelines* **1998**, *43*, 5–18.

14. Zhai, Y.H.; Guo, X.P.; Qu, L.S. Corrosion evaluation and remaining life prediction of gathering and transmission pipelines. *Oil Gas Field Surf. Eng.* **2006**, *25*, 47–48.
15. Hou, Y.H.; Li, Y.P. Effects of cold working on corrosion resistance of Co-modified Ni–16Cr–15Mo alloy in hydrofluoric acid solution. *Corros. Sci.* **2014**, *89*, 258–267. [CrossRef]
16. Hu, W. *Fluorine Chemical Production Technology*; Science Press: Beijing, China, 2010.
17. Wang, X.F. Analysis of HF acid regeneration tower wall corrosion defects and safety evaluation. *Petrochem. Corros. Prot.* **2013**, *30*, 52–54.
18. Wu, S. Corrosion failure analysis of alkyl benzene HF regeneration tower feed heater. *Mechatron. Prod. Dev. Innov.* **2010**, *23*, 78–79.
19. Zhang, W. Study of HF acid corrosion behavior of regeneration tower of alkyl benzene plant. *Pipeline Technol. Equip.* **2008**, *2*, 56–58.
20. Lv, E.W.; Li, W.C. Application of graphite lining technology in fluorine chemical projects. *Chem. Des.* **2017**, *4*, 19–23.
21. Zheng, G.T. Simulation study and optimization of vinylidene fluoride production process. *Chem. Prod. Technol.* **2011**, *18*, 11–14.
22. Xu, M.L. Process design of a production plant for monochlorodifluoroethane. *Chem. Eng. Equip.* **2015**, *10*, 53–62.
23. Jiang, H.L. Study on the optimization of hexafluoropropylene (HFP) distillation process. *Chem. Manag.* **2018**, *502*, 202–203.
24. Fang, Z.; Chen, R.X.; Wang, Z. Prediction method and application case analysis of dangerous parts of pipelines in petrochemical plants. In Proceedings of the ASME 2014 Pressure Vessels & Piping Conference, Virtual, Online, 13–15 July 2021.
25. Du, M.J.; Zhang, Z.T.; Zhang, C.Y. Analysis of erosion fracture stress of 90° elbow in multi-phase mixed transmission pipeline. *Oil Gas Storage Transp.* **2011**, *30*, 427–430.
26. Fang, Z.; Jia, G.D.; Liu, D.Y. Study on carburizing inspection of cracking furnace tube using acoustic emission technique. In Proceedings of the ASME 2014 Pressure Vessels & Piping Conference, Anaheim, CA, USA, 20–24 July 2014.